Contents

List of Figures

Introduction

Supply chains management represents one of the most important challenges in the industrial production context. The growth of competitiveness, in the vision of a globalized economic scenario, induced companies and managers to change their strategic positioning, reducing costs and improving product quality and offered services.

The concept of supply chain (SC) expresses a sequence of integrated operations and services ranging from the acceptance of consumers demand to the production and finally to delivery. Then, the trend of managers is to find new optimization techniques in order to improve the whole productive cycle and to maximize the total level of service, integrating informations between stakeholders, logistics and multimodal transports, and cash flows.

The main processes of a SC can be divided in:

- production planning and inventory control, i.e. creation of an asset, material procurement, manufacturing and assembly, and storage
- logistics, i.e. demand management and distribution to final clients.

In this context, one of the major issue is the definition of storage level of goods required to satisfy the market demand. So, stocks have a great importance for the life of companies, especially when the amount of required materials is uncertain, since from it companies can draw resources in emergency situations, avoiding to lose a slice of market. For this reason, the inventory management is a core activity which, however, can not be separated from the coordination of the flow of products and informations. In fact, if each entity of supply chain is not perfectly aligned and not has a correct vision of the customers demand, the level and typology of stocks may not be optimized causing negative effects, such as the "Forrester"

effect, known as *bullwhip*. This effect consists of an amplification of demand from downstream to upstream that a variation of 10% in the sales of retailers may cause a variation of more than 40% in demand of producers. It can be reduced if the information on consumption are carefully shared throughout the supply chain.

The importance of implementing strategies and policies for an efficient management of the supply chain has stimulated the interest of many researchers proposing different scientific approaches attempting to model and simulate the operational flow of the various stages of a production process. Then, the increasing technological innovations and the growth of ICT allowed managers to get software simulation tools supporting the decision process.

The main goal of this thesis is to present and implement some simulation models to show some critical phenomena appearing in planning and managing such systems in order to prevent the resulting negative effects.

In particular some macroscopic models for supply chains and networks able to reproduce the goods dynamics are discussed.

The analyzed macroscopic models are based on the conservation laws, which are represented by special partial differential equations where the variable is a *conserved quantity*, physically a quantity which can neither be created nor destroyed. The main idea is to look at large scales so to consider the processed parts as small particles which flow in a continuous way and to assume the conservation of their density.

Depending on the observation scale supply networks modeling is characterized by different mathematical approaches: discrete event simulations and continuous models. Since discrete event models (see [12]) are based on considerations of individual parts, their main drawback is, however, an enormous computational effort. Then a cost-effective alternative to them is continuous models, described by some partial differential equation. The first proposed continuous models date back to the early 60's and started with the work of [5] and [21], but the most significant in this direction was [11], where the authors, via a limit procedure on the number of parts and suppliers, have obtained a conservation law ([3], [10]), whose flux involves either the parts density or the maximal productive capacity.

Then, in recent years continuous and homogenous product flow models have been introduced, for example in [9], [11], [16], [23], [24], and they have been built in

close connection to other transport problems like vehicular traffic flow and queuing theory. Extensions on networks have been also treated in [15], [25], [26].

In this thesis, starting by the historical model of Armbruster - Degond - Ringhofer, we have compared two different macroscopic models, i.e. the Klar model, based on a differential partial equation for density and an ordinary differential equation to capture the evolution of queues, and a continuum-discrete model, formed by a conservation law for the density and an evolution equation for processing rate. Both the models can be applied for supply chains and networks.

A supply network is characterized by a set of interconnected suppliers which, in general, consist of a processor and, if we deal with the Klar model, a buffer or a queue. Each processor is characterized by a maximum processing rate μ_j, length L_j, and processing time T_j. The quantity $\frac{L_j}{T_j}$ represents the processing velocity. To study the dynamics at the connection points or junctions, some special parameters are introduced; in particular when the number of incoming suppliers is greater than the outgoing ones, we consider the priority parameters $(q_1, ..., q_n)$, where $q_i \in]0, 1[$ determines a *level of priority* at the junction of incoming suppliers, while, on the contrary, we consider the flux distribution parameters $(\alpha_1, ..., \alpha_m)$, where $\alpha_j \in]0, 1[$, with $\sum_{j=1}^{m} \alpha_j = 1$, indicates the percentage of parts addressed from an incoming supplier to an outgoing one. At junctions, a way to solve Riemann problems, i.e. Cauchy problems with constant initial data on each arc, is prescribed for the continuum-discrete model and a solution at junctions guaranteeing the conservation of fluxes is defined.

We have to notice some differences between the Klar and continuum-discrete model. In fact, the first one considers the formation and propagation of queue, under the assumption that the processing rate μ_j is constant, while the second one do not taking account of queues but describes the evolution of μ_j which is a time-spatial dependent function. It is evident that the two models complete each other. In fact, the approach of Klar is more suitable when the presence of queue with buffer is fundamental to manage goods production. On the other hand, the mixed continuum-discrete model is useful when there is the possibility to reorganize the supply chain, i.e when the productive capacity can be readapted for some contingent necessity. In order to make a comparison of the two models, some numerical results are shown via simulations.

Since the Armbruster and Klar models were defined taking into account an ideal queue, i.e. a buffer with infinity capacity, we analyzed the more realistic case in which a finite length buffer at each processor is considered. The finite size buffers lead to a discontinuous clearing function describing the throughput as a function of the Work In Progress (WIP), dependent on the production stage and decaying linearly as a function of the distance from the end of the production line. Then, starting from the Dallery and Gershwin's approach ([13]), we focused on a continuum model of a production line with finite buffers that allows us to study transient and other time dependent phenomena. In particular the interest is concerned in the time evolution of a major temporary shutdown of the production line due to a failure and the time evolution of the recovery of the production line once the failure has been repaired.

Chapter 1 presents the main macroscopic models for supply chains and networks, based on conservation laws. Chapter 2 is devoted to numerical methods used to discretize the proposed models in Chapter 1. In chapter 3, finally, we show some simulation results from the Klar and continuum-discrete models for both chains and networks.

Chapter 1

Macroscopic models for supply chain and networks

In this chapter, starting by the Armbruster-Degond-Ringhofer model, we present the Göttlich-Herty-Klar model and a continuum-discrete model for supply chains and networks.

1.1 The Armbruster-Degond-Ringhofer model

Consider a production line formed by M suppliers $S_0, ...S_M$, in which a certain good is processed by each supplier and is fed in the next one.

Labeling the processed part by index n, we denote by $\tau(m,n)$ the time at which the part n passes from $m-1$ to m supplier. Then, in order to model generic supply chain, the goal is to derive rules governing the evolution of each $\tau(m,n)$. A hierarchy of models is available for this purpose, but the focus is centralized on the so called fluid models, which replace the individual parts by a continuum and use rate equations for the flow of product through a supplier (see [1], [6] for an overview). For a large number of parts, these are computationally much less expensive than discrete event simulation models, but they necessarily represent an approximation to the actual situation.

Then we derive a fluid dynamic model, namely a conservation law for a partial differential equation, out of very simple principles governing the evolution of the times $\tau(m,n)$. Basically we assume that each supplier works as a single processor

characterized by its processing time $T(m)$ as well as its maximal production rate (capacity) $\mu(m)$ and a buffer queue in front of it. The processing policy is supposed to be 'first come first served'; $T(m)$ represents the time which is needed to produce a single part while $\mu(m)$ is defined as the maximal amount of parts per unit time which can handled by each single processor $m = 0, ...M-1$. In this model both $T(m)$ and $\mu(m)$ are fixed.

We denote by a_n, $n = 1, 2, ..$, the time part number n arrives at the end of queue and by b_n the 'release time', i.e. the time part number n reaches the front of the queue and is fed into the processor. If the queue is full, the interval between two consecutive times b_n will be given by the processing rate $\mu(m)$, i.e.

$$b_n = b_{n-1} + \frac{1}{\mu(m)}$$

will hold as long as $a_n \leq b_{n-1} + \frac{1}{\mu(m)}$ holds, meaning that part number n has already arrived when we want to feed it into the processor m. Instead, if the queue is empty, we wait that part n arrives to the end of queue and immediately feed it into the processor. In this case the condition $a_n > b_{n-1} + \frac{1}{\mu(m)}$ will imply $b_n = a_n$. Then, combining the two previous, we obtain the relation:

$$b_n = \max\left\{a_n, b_{n-1} + \frac{1}{\mu(m)}\right\}. \tag{1.1}$$

If $T(m)$ is the processing time to finish the part, we denote by $e_n = b_n + T(m)$ the time the part leaves the processor and enters the next queue. So, the (1.1) can be re-write as:

$$e_n = \max\left\{a_n + T(m), e_{n-1} + \frac{1}{\mu(m)}\right\}. \tag{1.2}$$

which represents the basic relationship between the arrival times a_n and the exit times e_n.

Referring now to the previous definition of $\tau(m, n)$ and using the obvious change of notation $a_n \to \tau(m, n)$ and $e_n \to \tau(m+1, n)$ we obtain from (1.2)

$$\tau(m+1, n) = \max\left\{\tau(m, n) + T(m), \tau(m+1, n-1) + \frac{1}{\mu(m)}\right\}, \tag{1.3}$$
$$n \geq 1,\ m = 0, .., M-1.$$

The (1.3) needs initial and boundary conditions which are:

$$\tau(0,n) = \tau^A(n),\ n \geq 0, \quad \tau(m,0) = \tau^I(m),\ m = 0,...M, \tag{1.4}$$

where $\tau^A(n)$ simply denotes the arrival time of part n in the first processor and $\tau^I(m)$ denotes the time the first part has arrived at supplier S_m. The (1.3) and (1.4) define completely a discrete event simulation model. So, $\tau^I(m+1) - \tau^I(m) - T(m)$ denotes the time the first part has waited in the buffer in front of processor at S_m, while, assuming a constant service rate μ in the past,
$\mu(m,0)\left[\tau^I(m+1) - \tau^I(m) - T(m)\right]$ would be the number of parts in the queue at the time part number 0 arrives. This definition indicates that, for an actual simulation, we have to start somewhere. But this issue will be resolved once the problem is formulated in terms of a conservation law. Then, given the times $\tau(m,n)$, conservation of the number of parts is expressed via the introduction of the Newell-curves (see [11], [31]), which describe how the information of (1.3) can be organized to facilitate the computation of performance measures, e.g. the Work in Progress (WIP). In this context, the N-curve $U(m,t)$ at supplier S_m is given by the number of parts which have passed from processor S_{m-1} to S_m at any time t, i.e by

$$U(m,t) = \sum_{n=0}^{\infty} H(t - \tau(m,n)),\ t > 0, \tag{1.5}$$

where H is the Heavyside function, i.e.

$$H(y) = \begin{cases} 0 & if\ y < 0 \\ 1 & if\ \ y \geq 0 \end{cases}.$$

The WIP $W(m,t)$ of processor S_m, the total number of parts (including all parts in the queue as well) actually produced at S_m at time t, is given by the difference of two consecutive N-curves:

$$W(m,t) = U(m,t) - U(m+1,t) + K(m),\ \ m = 0,...M, \tag{1.6}$$

where the time independent constants $K(m)$ are determined by initial situation. If each of processors S_m has a given minimal processing time $T(m)$ then

$\tau(m+1,n) \geq \tau(m,n) + T(m)$ will hold and this implies that $W(m,t)$ can never become negative.

Considering the first derivative of $W(m,t)$ with respect to t, we obtain:

$$\begin{aligned} \frac{d}{dt}W(m,t) = \frac{d}{dt}U(m,t) - \frac{d}{dt}U(m+1,t) = \\ \sum_{n=0}^{\infty}\delta(t-\tau(m,n)) - \sum_{n=0}^{\infty}\delta(t-\tau(m+1,n)) = \\ = F(m,t) - F(m+1,t), \end{aligned} \tag{1.7}$$

where, by definition, the flux $F(m,t)$ from processor S_{m-1} to S_m is given by the first derivative of $U(m,t)$ and it can be interpreted as a superposition of δ-distributions. To avoid this inconvenience, the (1.7) is replaced by a conservation law with a simple constitutive relation between the density ρ and the flux f, in which continuous averaged quantities are considered and the dependence on individual parts is completely removed.

By a reformulation of the problem, necessary to prevent analytical difficulties, it can be shown that the asymptotic limit leads to a partial differential equation. First, we map (1.7) onto a grid in an artificial spatial variable x, called the 'Degree of Completion' (DOC). We define a mesh $0 = x_0 < ..... < x_M = X$ and replace $F(m,t)$ by $F(x_m,t)$. So the parts enter and leave the supply chain respectively at the DOC $x = 0$ and DOC $x = X$. Next, multiplying the flux by an arbitrary smooth test function $\psi(t)$, the integral

$$\int_{\tau^I(m)}^{\infty}\psi(t)F(x_m,t)\,dt = \sum_{n=0}^{\infty}\int_{\tau^I(m)}^{\infty}\psi(t)\delta(t-\tau(m,n))\,dt = \sum_{n=0}^{\infty}\psi(\tau(m,n)) \tag{1.8}$$

holds. Then we can rewrite the (1.8) into a Riemann sum as

$$\int_{\tau^I(m)}^{\infty}\psi(t)F(x_m,t)\,dt = \sum_{n=0}^{\infty}\psi(\tau(m,n))\,\Delta_n\tau(m,n)\,f(x_m,\tau(m,n))$$

where the increment is given by the difference of $\tau(m,n)$ in the index n, i.e. $\Delta_n\tau(m,n) = \tau(m,n+1) - \tau(m,n)$, and, as consequence from (1.8), the function

$f(x_m, \tau(m,n))$ is provided by the inverse of $\Delta_n\tau(m,n)$. For a $\Delta_n\tau(m,n)$ small, i.e. $\Delta_n\tau(m,n) \to 0$, we obtain the approximate relation

$$\int_{\tau^I(m)}^{\infty} \psi(t) F(x_m, t)\, dt \approx \int_{\tau^I(m)}^{\infty} \psi(t) f(x_m, t)\, dt$$

where the function f is the approximate flux for $t = \tau(m,n)$ and $x = x_m$, i.e.

$$f(x_m, \tau(m,n)) = \frac{1}{\tau(m,n+1) - \tau(m,n)}, \qquad n \geq 0,\ m = 0, ..., M. \tag{1.9}$$

Assuming now that the arrival times τ are continuously distributed, i.e. expressed in terms of continuous variables such as $\tau(x,y)$, we rewrite the approximate flux as $f(x, \tau(x,y)) = \frac{1}{\partial_y \tau(x,y)}$. In the similar way, it is possible to find an approximation of part density ρ.

We can observe that the N-function $U(x,t)$, the antiderivative of the flux, satisfies the relations

$$\begin{aligned} &(a)\ \frac{d}{dy} U(x, \tau(x,y)) = \partial_t U(x,\tau)\, \partial_y \tau = 1, \\ &(b)\ \frac{d}{dx} U(x, \tau(x,y)) = \partial_x U(x,\tau) + \partial_t U(x,\tau)\, \partial_x \tau. \end{aligned} \tag{1.10}$$

In analogy to (1.6) setting $\rho(x,t) = K(x) - \partial_x U(x,t)$, with K an arbitrary function, and since $\partial_t U(x,\tau) = f(x,\tau)$, the (1.10) becomes

$$\frac{d}{dx} U(x, \tau(x,y)) = K(x) - \rho(x,t) + f(x,\tau)\, \partial_x \tau.$$

Moreover the (1.10-a) implies that $\frac{d}{dy} U(x, \tau(x,y))$ can be set to an arbitrary chosen function $K(x)$, since it is a function of the DOC variable x only. So for a continuum $\tau(x,y)$ we set $\rho(x,t) = \frac{\partial_x \tau}{\partial_y \tau}$. ρ and f satisfy a conservation law of the form $\partial_t \rho + \partial_x f = 0$.

Thus, on a discrete level, the approximate density is given by

$$\rho(x_m, \tau(m+1,n)) = \frac{\tau(m+1,n+1) - \tau(m,n+1)}{h_m\left(\tau(m+1,n+1) - \tau(m+1,n)\right)} \tag{1.11}$$

with $n \geq 0$, $m = 0, ..., M-1$, $h_m := x_{m+1} - x_m$.

The definitions in (1.9) and (1.11) allow to derive a simple constitutive relation between flux and density as shown in the following theorem.

Theorem 1 *Let the arrival times $\tau(m,n)$ satisfy the time recursion (1.3) and let the approximate density ρ and flux f be defined by (1.11) and (1.9). Then the approximate flux can be written in terms of the approximate density via a constitutive relation of the form*

$$f(x_m, \tau(m,n)) = \min\left\{\mu(m-1,n), \frac{h_{m-1}\rho(x_{m-1}, \tau(m,n))}{T(m-1)}\right\},$$

with $n \geq 0$, $m = 1, 2, ...$

Proof. The proof was done by Armbruster et al. and it can be found in [2]. ■

Now, it will be shown that the approximate density ρ and flux f, defined by (1.11) and (1.9), satisfy a conservation law of the form $\partial_t \rho + \partial_x f = 0$, asymptotically, i.e. for a large time and nodes scales ($N, M \to \infty$). Moreover the asymptotic validity can be divided into three parts: scaling, interpolation and weak formulation.

1.1.1 Scaling and dimensionless formulation

We define the average processing time T_0 as

$$T_0 = \frac{1}{M}\sum_{m=0}^{M-1} T(m),$$

and so MT_0 describes the time a part spent to be processed in the empty system without any waiting times. Then, T_0 is used as a scale basis over all time scales, and we denote all scaled variables and functions by the subindex s.

$$\tau(m,n) = MT_0\tau_s(m,n), \quad T(m) = T_0 T_s(x_m), \quad \mu(m,n) = \frac{\mu_s(x_m, \tau_s(m+1,n))}{T_0}. \tag{1.12}$$

Consider a regime where $M >> 1$ and set $\varepsilon = \frac{1}{M} << 1$. Inserting (1.12) into (1.3), for $n = 0, 1, ..$ and $m = 0, ..M-1$ we get:

$$\tau_s(m+1,n+1) = \max\left\{\tau_s(m,n+1) + \varepsilon T_s(x_m), \tau_s(m+1,n) + \frac{\varepsilon}{\mu_s(x_m, \tau_s(m+1,n))}\right\}, \tag{1.13}$$

where the initial and boundary condition, respectively $\tau_s^A = \tau_s(0,n)$ and $\tau_s^I = \tau_s(m,0)$, are scaled in the same way as $\tau(m,n)$.

It is assumed that the differences between two consecutive arrival times τ are of the same order as the average processing time T_0. This is reasonable since otherwise the total WIP would either go to zero or infinity. So it is set

$$\Delta_n\tau(m,n) = \tau(m,n+1) - \tau(m,n) = T_0\Delta_{ns}\tau_s(m,n),$$
$$\Delta_m\tau(m,n) = \tau(m+1,n) - \tau(m,n) = T_0\Delta_{ms}\tau_s(m,n),$$

giving

$$\tau_s(m+1,n) = \tau_s(m,n) + \varepsilon\Delta_{ms}\tau_s(m,n),$$
$$\tau_s(m,n+1) = \tau_s(m,n) + \varepsilon\Delta_{ns}\tau_s(m,n).$$

Then, scaling the density ρ (1.11) and the flux f (1.9) we get

$$f(x,t) = \frac{1}{T_0} f_s\left(x, \frac{t}{MT_0}\right),$$
$$\rho(x,t) = \frac{M}{X}\rho_s\left(x, \frac{t}{MT_0}\right),$$

where X is the length of the DOC interval. Finally

$$\begin{aligned} &f_s(x_m, \tau_s(m,n)) = \tfrac{1}{\Delta_{ns}\tau_s(m,n)}, && m = 0,..,M,\ n = 0,1,.. \\ &\rho_s(x_m, \tau_s(m+1,n)) = \tfrac{\varepsilon X\Delta_{ms}\tau_s(m,n+1)}{h_m\Delta_{ns}\tau_s(m+1,n)}, && m = 0,..,M,\ n = 0,1,... \end{aligned} \tag{1.14}$$

1.1.2 Interpolation and weak formulation

In this section, it will be show the asymptotic validity of a conservation law in the regime situation, which is considered supposing $M >> 1$ or $\varepsilon = \frac{1}{M} << 1$. The goal is an initial boundary value problem for the conservation law

$$\partial_t \rho + \partial_x f = 0, \quad f = \min\left\{\mu\left(x,t\right), \rho\right\}, \quad f\left(0,t\right) = f^A\left(t\right), \tag{1.15}$$

together with some initial condition $\rho\left(x,0\right) = \rho_0\left(t\right)$.

Several complications appear in this approach; in fact, the main difficulty arising from $M \to \infty$, or equivalently $\varepsilon \to 0$, is that the flux function f can become discontinuous due to the assumption of different maximal capacities. Consider the following bottleneck scenario: if processor x_m has a higher capacity than x_{m+1}, i.e. $\mu\left(x_{m+1}\right) < \mu\left(x_m\right)$, a queue in front of x_{m+1} will grow. But, since mass still has to be conserved, this discontinuity has to be compensated by a δ-distribution in the density ρ which, hence, will not be a classical function. To deal with this issue, an asymptotic analysis for the Newell-curve $U\left(m,t\right)$ (1.5) is performed. Denoting the approximation of U by u, setting $\rho\left(x,t\right) = -\partial_x u\left(x,t\right)$ and integrating the (1.15) once respect to x, we get

$$\partial_t u\left(x,t\right) - \min\left\{\mu\left(x,t\right), -\partial_x u\right\}, \quad \lim_{x \to 0^-} u\left(x,t\right) = g^A\left(t\right), \quad \frac{d}{dt} g^A\left(t\right) = f^A\left(t\right) \tag{1.16}$$

The last equation allows for shock solutions appearing as a δ-distribution in u. In this case, although the x-derivative of u becomes unbounded, the flux (i.e. $\partial_t u\left(x,t\right)$) will be bounded because of the $min-$function. It is possible to show that, in the limit $\varepsilon \to 0$, u satisfies the hyperbolic problem in (1.16) weakly in space x and time t. First we have to define the interpolating elements in the form of scaled functions $\widetilde{u}_s$ and $\widetilde{f}_s$. An effective method towards a continuum is a piecewise constant interpolation in space and time. Then, the next theorem will show that the N-curve $\widetilde{u}_s$ satisfies the (1.16) weakly in x and t as $\varepsilon \to 0$.

Theorem 2 *Given the scaled density and flux at the discrete points $x_m, \tau_s\left(m,n\right)$, as defined in (1.13). Let the scaled throughput times $T_s\left(x_m\right)$ stay uniformly bounded, i.e. $h_m = O\left(\varepsilon\right)$ holds uniformly in m. Assume finitely many bottlenecks for a finite amount of time, i.e. let $\Delta_m \tau_s\left(m,n\right)$ be bounded for $\varepsilon \to 0$ expect for a certain number of nodes m and a finite number of parts n, which stays bounded as $\varepsilon \to 0$. Then, for $\varepsilon \to 0$, and $\max h_m \to 0$ the interpolated N-function and flux*

$\widetilde{u}_s$, $\widetilde{f}_s$ satisfy the initial boundary value problem

$$\partial_t \widetilde{u}_s = \widetilde{f}_s, \quad \widetilde{f}_s = \min\left\{\mu, -\partial_x \widetilde{u}_s\right\}, \quad t > \widetilde{\tau}_s^I(x), \quad 0 < x < X, \tag{1.17}$$
$$\widetilde{u}_s\left(x, \widetilde{\tau}_s^I(x)\right) = 0, \quad \lim_{x\to 0^-} \widetilde{u}_s(x,t) = \int_{\widetilde{\tau}_s(0,0)}^{t} f^A(s)\, ds$$

in the limit $\varepsilon \to 0$, weakly in x and t.

Proof. The proof was done by Armbruster et al. and it can be found in [2]. ■

Then, through this theorem, it is proved the asymptotic validity of the integrated conservation law (1.17), for any N-curve u and any flux f, derived from an arbitrary sequence τ via the definitions (1.9) and (1.11) and the interpolating elements $\widetilde{u}_s$, $\widetilde{f}_s$.

Moreover, considering the unscaled variables, Theorem (2) implies that density $\rho(x,t)$ can be approximately computed as $\rho = -\partial_x u$.

1.2 The Armbruster-Göttlich-Herty model with finite buffers

Let consider an $M/M/1$ queue, from elementary queueing theory, the mean cycle-time through the queue is given by $\tau = \frac{1}{\nu-\lambda}$ where ν is the average processing rate, identical for all processors, and λ is the arrival rate of parts. Calling ρ the average number of parts in the queueing system, Little's law becomes $\lambda\tau = \rho$, and solving for λ, the clearing function is

$$\lambda = \frac{\nu\rho}{1+\rho} \tag{1.18}$$

If we identify λ with the steady state flux F and ρ with the amount of WIP in the production process, the equation (1.18) is the state equation for our PDE (Partial Differential Equation) model and the $M/M/1$ clearing function is the same used in [2]. Moreover Little's law [30] still holds true and hence the structure of the model is still a conservation law as

$$\rho_t + F_x = 0, \ x \in [0,1], \ t \geq 0 \tag{1.19}$$

where $\rho(x,t)$ is the density with maximum value M and F is the flux.

Let observe that the probability to move through the generic jth processor and arrive at the $(j+1)th$ one depends on two stochastic processes:

- the exponentially distributed departure time process with a mean of ν;
- the buffer levels process, i.e. the probabilities that the buffer level become M and hence the $j+1$ buffer is full and the jth processor has to be idle.

Let assume that the probability the next buffer is full linearly increases with the distance from the end of production line. In particular, that probability is zero for the last processor since it feeds the outside and it is assumed an infinite outside inventory. Then, based on this assumptions, the processing rate becomes inhomogeneous of the form $\widetilde{v} = c(x)\nu$, where $c(1) = 1$, $c(x)$ linearly increases with the steady state influx λ and linearly decreases as a function of x. Concerning with all three assumptions, we get

$$\widetilde{v} = c(x)\nu = \lambda k(x-1) + \nu,$$

where $k > 0$ is the decay rate of $\widetilde{v}$ along x, and it is a monotone increasing function of M. As done to find (1.18), the clearing function is given by

$$F(\rho, x) = \begin{cases} \frac{\nu\rho}{1+\rho+k\rho(1-x)} & \rho < M \\ 0 & \rho \geq M \end{cases} \tag{1.20}$$

Both (1.18) and (1.20) have to be completed with suitable boundary conditions.

1.2.1 Boundary conditions

An inflow $\lambda(t)$ at $x = 0$ and an outflow $\mu(t)$ at $x = 1$ is assigned. Due to the lack of monotonicity of F we might not be able to fulfill the conditions $\lambda(t) = F(\rho(0,t),0)$ and $\mu(t) = F(\rho(1,t),1)$ at each time instant t. So, we use the weak formulations as in [4].

We denote by $\rho(0+,t) = \lim_{x\to 0, x\geq 0}\rho(x,t)$ and $\rho(1-,t) = \lim_{x\to 1, x\leq 1}\rho(x,t)$. Let $\rho_\lambda \in [0, M)$ be the unique density such that

$$F(\rho_\lambda, 0) = \lambda, \tag{1.21}$$

and $\rho_\mu \in (0, M]$ such that

$$F(\rho_\mu, 0) = \mu. \tag{1.22}$$

Then, the following boundary conditions are hold.

$$\max_{k \in I(\rho_\lambda(t), \rho(0+,t))} \{sgn(\rho(0+,t) - \rho_\lambda(t))(F(\rho(0+,t),0) - F(k,0))\} = 0 \tag{1.23}$$

$$\max_{k \in I(\rho_\mu(t), \rho(0+,t))} \{sgn(\rho(1-,t) - \rho_\mu(t))(F(\rho(1-,t),1) - F(k,1))\} = 0 \tag{1.24}$$

We can notice that these two conditions are consistent with the behaviour of supply chains. In fact, for example, if $\rho(0+,t) = M$, then (1.23) holds true independent from the choice of ρ_λ, and it means that no more parts can enter the supply chain. But, if $\rho(0+,t) < M$, (1.23) implies that $\rho(0+,t) = \rho_\lambda$ or $F(\rho(0+,t),0) = \lambda$.

1.2.2 Steady states

Through the boundary conditions, it is possible to compute the WIP profiles in equilibrium. In steady state we have

$$\frac{\partial F(\rho(x), x)}{\partial x} = 0 \tag{1.25}$$

and hence

$$F(\rho(x), x) = c, \tag{1.26}$$

where the constant c is given by the boundary conditions (1.23) and (1.24) at $x = 0$ and $x = 1$, respectively.

$\rho(x) = 0$ is a steady state if and only if $\rho_\lambda = 0$ and this state satisfies the boundary condition at $x = 1$ for any boundary density ρ_μ. If at some point x_0 we have $\rho(x_0) = M$, then $c = 0$, necessarily. Hence, (1.26) implies that at any other point x we either have $\rho(x) = 0$ or $\rho(x) = M$, and the only continuous steady state in this case is $\rho(x) = M$, satisfying the boundary condition at $x = 0$ for any incoming density ρ_λ implying $\rho_\mu = M$.

If $0 < \rho < M$ for all x, the (1.24) is satisfied for all ρ_μ and $\rho(x=0) = \rho_\lambda$ defines $c = \frac{\nu\rho_\lambda}{1+\rho_\lambda(1+k)}$. Since $F(\rho, x)$, defined as in (1.20), is strictly monotone in ρ for all x, then

$$\rho(x) = F^{-1}(c, x) = -\frac{c}{c(1+k-kx)-\nu}, \tag{1.27}$$

which is the well-defined steady state.

Finally we get the following result.

Proposition 3 *Consider the conservation law (1.19) with flux function (1.20) and boundary conditions as in (1.23) and (1.24). Assume inflow λ and outflow μ are such that ρ_λ (1.21) and ρ_μ (1.22) are well defined. Then, there exist three continuous steady states $x \to \rho(x)$ of the conservation law: i) If $\mu = 0$ and $\lambda = 0$, then $\rho = 0$; ii) if $\mu = 0$ and $\lambda > 0$, then $\rho = M$; iii)in all other cases the steady state is given by equation (1.27).*

1.2.3 Riemann Problem

Taking into account the discontinuity in the flux function and neglecting the dependence of the flux on x, the conservation law can be write as

$$\rho_t + \partial_x H(M-\rho) f(\rho) = 0, \tag{1.28}$$

where f is some strictly monotone and smooth function and $H(\cdot)$ represents the Heaviside function.

To capture the dynamics of (1.28), we study the associated Riemann problem, which is a Cauchy problem with the following initial condition

$$\rho(x) = \begin{pmatrix} \rho_l & x < 0 \\ \rho_r & x > 0 \end{pmatrix} \tag{1.29}$$

where ρ_l and ρ_r are constant.

Starting from the topics discussed in [17], [18], [19], [20] about entropic solution , if we apply this notion to the case $H(M-\rho) f(\rho)$, we can characterize the solutions of (1.28) as follows:

- For $0 \leq \rho_l < \rho_r < M$, the solution is a classical shock wave with speed $s = \frac{f(\rho_r)-f(\rho_l)}{\rho_r-\rho_l}$.

- For $0 \leq \rho_r < \rho_l < M$, the solution is a classical rarefaction wave traveling with speed $\widetilde{s} = f'(\rho)$.
- For $0 \leq \rho_l < \rho_r = M$, the solution is again a shock wave traveling with speed $s = \frac{f(\rho_l)}{\rho_l - M}$.
- For $0 \leq \rho_r < \rho_l = M$ (this case is not covered in [18]), the solution is a wave with speed negative infinity connecting the points $(M, 0)$ and $(M, f(M))$ in the phase space $\rho - \rho\nu$. This wave is followed by a classical rarefaction wave of positive speed connecting on the left $(M, f(M))$ to $(\rho_r, f(\rho_r))$.

1.3 The Göttlich-Herty-Klar model

In this section, we present a model for large queuing supply chain networks based on the work of Armbruster, Degond and Ringhofer [2]. Mainly, we formulate a PDE network problem and a separate modeling of the queues, taking advantage of existence theory of the network problem.

First, we state the definition of a supply chain network describing the connection between it and the suppliers.

Definition 4 . *A supply chain network is a finite, connected directed, simple graph consisting of arcs $J = \{1, ..., N\}$ and vertices $V = \{1, ..., N-1\}$. Each supplier j is modeled by an arc j, which is again parameterized by an interval $[a_j, b_j]$. We use $a_1 = -\infty$ and $b_N = +\infty$ for the first respectively the last supplier in the supply chain.*

First we consider the special case where each vertex is connected to exactly two arcs. As shown in Fig.1.1, we conventionally assume that $b_j = a_{j-1}$. Then, we state that a supplier j is defined by a processor and a queue in front of it, i.e. at $x = a_j$ (for simplicity we assume that the first supplier consists of a processor only).

Each processor j is characterized by a maximum processing capacity μ_j, its length L_j and the processing time T_j. The rate $\frac{L_j}{T_j}$ defines the processing velocity. The evolution of parts inside the processor j is modeled by the function $\rho_j(x, t)$ indicating the density of parts in j at point x and time t.

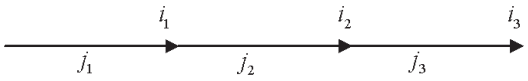

Figure 1.1: Example of a simple network structure.

The dynamics of each processor on an arc j are governed by the following advection equation:

$$\begin{cases} \partial_t \rho_j(x,t) + \partial_x \min\left\{\mu_j, \frac{L_j}{T_j}\rho_j(x,t)\right\} = 0, & \forall x \in [a_j, b_j],\ t \in \mathbb{R}^+ \\ \rho_j(x,0) = \rho_{j,0}(x), & \forall x \in [a_j, b_j] \end{cases} \tag{1.30}$$

Note that we use the flux functions defined as

$$f : \mathbb{R}_0^+ \to [0,\mu], \quad f(\rho) = \min\left\{\mu, \frac{L}{T}\rho\right\}, \tag{1.31}$$

where the maximal rate for the processor is a positive constant μ. Clearly, f is Lipschitz with constant $L_f = \frac{L}{T}$.

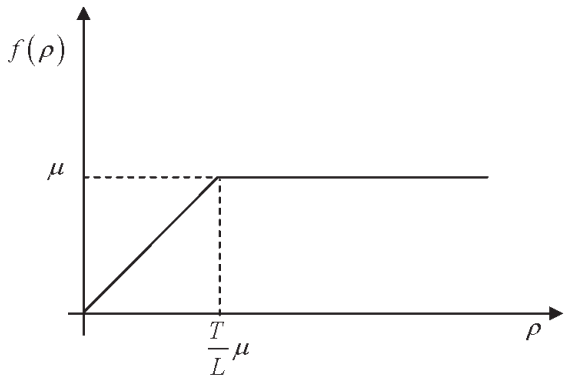

Figure 1.2: Relation between flow and density.

Remark 5 *Usually, an inflow profile $f_1(t)$ for the supply chain is given. This profile can be translated into initial data $\rho_1(x,0) := \rho_{1,0}(b_1 - t) = f_1(t)$ on artificial first arc, where it's assumed $\mu_1 > \max f_1$ and $\frac{L_1}{T_1} = 1$.*

Each queue is a time-dependent function $t \to q_j(t)$ and buffered demands for the generic processor j when the capacity of processor $j-1$ is different from the demand of processor j (in fact, in this case the queue q_j increases or decreases its buffer).

Mathematically, we require each queue q_j to satisfy the following equation:

$$\partial_t q_j(t) = f_{j-1}(\rho_{j-1}(b_{j-1}, t)) - f_j(\rho_j(a_j, t)), \quad j = 2, ..., N \tag{1.32}$$

Due to the advection, we can define the flux on the outgoing arc j as

$$f_j(\rho_j(a_j, t)) = \begin{cases} \min\{f_{j-1}(\rho_{j-1}(b_{j-1}, t)), \mu_j\} & q_j(t) = 0 \\ \mu_j & q_j(t) > 0 \end{cases} \tag{1.33}$$

where the flux $f_j(\rho_j(a_j, t))$ is dependent on the capacity of the queue. The (1.33) allows for the following interpretation: if the outgoing buffer is empty, we process as many parts as possible but at most μ_j, while if it contains some parts, then we process at maximal possible rate, i.e. again μ_j.

Finally, we have the following coupled system of partial and ordinary differential equations on a network

$$\partial_t \rho_j(x, t) = -\partial_x \min\left\{\mu_j, \frac{L_j}{T_j}\rho_j(x, t)\right\} \tag{1.34}$$

$$\rho_j(x, 0) = \rho_{j,0}(x) \tag{1.34}$$

$$\partial_t q_j(t) = f_{j-1}(\rho_{j-1}(b_{j-1}, t)) - f_j(\rho_j(a_j, t)) \tag{1.35}$$

$$q_j(0) = q_{j,0} \tag{1.36}$$

$$f_j(\rho_j(a_j, t)) = \begin{cases} \min\{f_{j-1}(\rho_{j-1}(b_{j-1}, t)), \mu_j\} & q_j(t) = 0 \\ \mu_j & q_j(t) > 0 \end{cases} \tag{1.37}$$

Consider the very special flux function in (1.31), the Riemann problem for (1.30) and $(x, t) \in \mathbb{R} \times \mathbb{R}^+$ admits one of the following two solutions. Let the initial data such as

$$\rho_{j,0}(x) = \begin{cases} \rho_l & \text{for } x < 0 \\ \rho_r & \text{for } x \geq 0 \end{cases},$$

with $\rho_l, \rho_r \in \mathbb{R}_0^+$. Then, for $\rho_l < \rho_r$ the solution ρ_j is given by

$$\rho_j(x,t) = \begin{cases} \rho_l & -\infty < \frac{x}{t} \leq \frac{f_j(\rho_r)-f_j(\rho_l)}{\rho_r-\rho_l} \\ \rho_r & \frac{f_j(\rho_r)-f_j(\rho_l)}{\rho_r-\rho_l} < \frac{x}{t} < \infty \end{cases} \tag{1.38}$$

while for $\rho_r < \rho_l$, if $\rho_l \leq \mu_j$ or $\rho_r \geq \mu_j$ the solution is the same, i.e. (1.38). Otherwise, in the case $\rho_r < \mu_j < \rho_l$, the solution will be

$$\rho(x,t) = \begin{cases} \rho_l & -\infty < \frac{x}{t} \leq \frac{f_j(\rho_l)-\mu_j}{\rho_l-\mu_j} \\ \mu_j & \frac{f_j(\rho_l)-\mu_j}{\rho_l-\mu_j} < \frac{x}{t} \leq \frac{\mu_j-f_j(\rho_r)}{\mu_j-\rho_r} \\ \rho_r & \frac{\mu_j-f_j(\rho_r)}{\mu_j-\rho_r} < \frac{x}{t} < \infty \end{cases} \tag{1.39}$$

where it holds $\frac{\mu_j-f_j(\rho_r)}{\mu_j-\rho_r}$ and $\frac{f_j(\rho_l)-\mu_j}{\rho_l-\mu_j} = 1$.

We can introduce the following definition:

Definition 6 (Network solution) *A family of functions $\{\rho_j, q_j\}_{j\in J}$ is called an admissible solution for a network as in 1.1 if, for all j, ρ_j is a weak entropic solutions [28] to (1.30), q_j is absolutely continuous and, in the sense of traces for $\rho_j s$, equations (1.32) and (1.33) hold for a.e. t.*

In particular, considering a single vertex $v \in V$ with incoming arc $j = 1$ and outgoing arc $j = 2$ and constant initial data $\rho_{j,0}(x) \leq \mu_j$, there exists an admissible solution $\{\rho_1, \rho_2, q_2\}$ which has the form:

$$\rho_1(x,t) = \rho_{1,0} \tag{1.40}$$

$$\rho_2(x,t) = \begin{cases} f_1(\rho_{1,0}) < \mu_2 \begin{cases} \rho_{1,0} & 0 \leq \frac{x-t_0}{t} < 1 = \frac{f_2(\mu_2)-f_2(\rho_{1,0})}{\mu_2-\rho_{1,0}} \\ \mu_2 & 1 \leq \frac{x-t_0}{t} \text{ and } \frac{x}{t} < 1 \\ \rho_{2,0} & 1 \leq \frac{x}{t} < \infty \end{cases} \\ f_1(\rho_{1,0}) \geq \mu_2 \begin{cases} \mu_2 & 0 \leq \frac{x}{t} < 1 = \frac{f_2(\mu_2)-f_2(\rho_{2,0})}{\mu_2-\rho_{2,0}} \\ \rho_{2,0} & 1 \leq \frac{x}{t} < \infty \end{cases} \end{cases} \tag{1.41}$$

$$q_2(t) = q_{2,0} + \int_0^t f_1(\rho_{1,0}) - f_2(\rho_2(a_2+,\tau))\, d\tau \tag{1.42}$$

where $t_0 = \frac{q_{2,0}}{\mu_2 - f_1(\rho_{1,0})}$.

For a network as in Fig.1.1 with initial values $q_j(0) = 0$ and initial data $\{\rho_{j,0}(x)\}_j$ where each $\rho_{j,0}$ is a step function, there exists an admissible solution $\{\rho_j, q_j\}_j$ to the network problem (1.34) to (1.37) whose construction is based on wave-front tracking algorithm.

1.3.1 Modeling general networks

Consider now a generic vertex $v \in V$ with m_v incoming and n_v outcoming arcs (as, for example, in Fig.1.3).

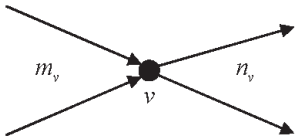

Figure 1.3: Geometry of a vertex with multiple incoming and outcoming arcs.

We denote by δ_v^- and δ_v^+ the set of arc indexes of incoming and outcoming arcs. If we have more than one outgoing arc, we need to define and successively to model the distribution of the goods from the incoming arcs. Assuming that for each vertex v a matrix $A_v := A(\alpha_{i,j}) \in \mathbb{R}^{m_v \times n_v}$ is given, hence, the total flux willing to go to arc $j \in \delta_v^+$ is given by

$$\sum_{i \in \delta_v^-} \alpha_{i,j} f_i(\rho_i(b_i-, t)).$$

Moreover we assume that, for all $i \in \delta_v^-$ and $j \in \delta_v^+$, the matrix A satisfies:

$$0 \leq \alpha_{i,j} \leq 1,$$

$$\sum_{j \in \delta_v^+} \alpha_{i,j} = 1.$$

Then, the supply chain network is modeling by (1.30) and,for each junction (vertex) v, by the following equation for the queues

$$\forall j \in \delta_v^+ \ : \ \partial_t q_j(t) = \sum_{i \in \delta_v^-} \alpha_{i,j} f_i(\rho_i(b_i-, t)) - f_j(\rho_j(a_j+, t)), \tag{1.43}$$

and the boundary values $\forall j \in \delta_v^+$,

$$f_j(\rho_j(a_j+, t)) = \begin{cases} \min\left\{\sum_{i \in \delta_v^-} \alpha_{i,j} f_i(\rho_i(b_i-, t)), \mu_j\right\} & q_j(t) = 0 \\ \mu_j & q_j(t) > 0 \end{cases}. \tag{1.44}$$

Starting by the empty queue, if the outgoing flux is a percentage of the sum of all incoming fluxes given by A_v the queue remains empty, while if it is equal to the maximal processing capacity, the queue increases. Finally if the queue is full, it is always reduced with a capacity determined by A_v and the capacities of the connected arcs.

Note that due to the positive velocity of the occurring waves the boundary conditions are well-defined. Moreover, due to (1.43) and the assumptions on A, the total flux at each vertex v is conserved for all times $t > 0$, i.e.

$$\sum_{j \in \delta_v^+} (\partial_t q_j(t) + f_j(\rho_j(a_j+, t))) = \sum_{i \in \delta_v^-} f_i(\rho_i(b_i-, t)).$$

The construction of a solution to the network problem given by (1.30), (1.43), (1.44) is as before.

Now, let $\eta = \min_j(b_j - a_j)$ be the minimum length of a supplier; since all waves move at positive velocity at most equal to 1, two interactions with vertices of the same wave can happen at most every η units of time. If N is the number of suppliers, than there is at most a multiplication by N every η unit of time, thus we can control the number of waves and interactions.

Therefore, for given piecewise constant initial data $\rho_{j,0}^\delta$ on a network, a solution $\left(\rho^\delta, q^\delta\right)$ can be defined by the wave-tracking method up to any time T.

1.4 A continuum-discrete model for supply chain network

In this section we introduce a supply chains model extending the Armbruster, Degond and Ringhofer one presented in the section 2.1, in which each arc is modeled by a conservation law for the good density ρ and an evolution equation for the processing rate μ.

Starting by the approach used in [14], once introduced the model, we discuss about possible choices of solutions at nodes guaranteeing the conservation of fluxes given by the general equation

$$\rho_t + f_\varepsilon(\rho, \mu)_x = 0,$$

where, for $\varepsilon > 0$ the flux f_ε is given by:

$$f_\varepsilon(\rho, \mu) = \begin{cases} m\rho, & if\ \rho \leq \mu, \\ m\mu + \varepsilon(\rho - \mu), & if\ \rho \geq \mu, \end{cases}$$

with m the processing velocity.

Keeping the analogy to Riemann problems, we call the solutions at junctions as Riemann Solver at nodes. The first choice is to fix the rule:

SC1 The incoming density flux is equal to the outgoing density flux. So, if a solution with only waves in the density ρ exists, then such solution is taken, otherwise the minimal μ wave is produced.

Rule **SC1** corresponds to the case in which processing rate adjustments are done only if necessary, while the density ρ can be regulated more freely. In particular, it is justified in all situations in which processing rate adjustments require re-building of the supply chain, while density adjustments are operated easily (e.g. by stocking).

Even if rule **SC1** is the most natural also from a geometric point of view, in the space of Riemann data, it produces waves only to lower the value of μ and this involves, as consequence, that, in some cases, the value of the processing rate does not increase and it is not possible to maximize the flux.

In order to avoid this problem, two additional rules to solve dynamics at a node are analyzed:

SC2 The objects are processed in order to maximize the flux with minimal value of the processing rate.

SC3 The objects are processed in order to maximize the flux. Then, if a solution with only waves in the density ρ exists, then such solution is taken, otherwise the minimal μ wave is produced.

The Riemann Problems are solved fixing two "routing" algorithms:

RA1 Goods from an incoming arc are sent to outgoing ones according to their final destination in order to maximize the flux over incoming arcs. Goods are processed ordered by arrival time (FIFO policy).

RA2 Goods are processed by arrival time (FIFO policy) and are sent to outgoing arcs in order to maximize the flux over incoming and outgoing arcs.

For both routing algorithms the flux of goods is maximized considering one of the two additional rules, **SC2** and **SC3**.

In order to understand the mechanism of the two previous rules, a simple example is shown.

Suppose to have a supply chain network for assembling orange and lemon fruit juice bottles as in Fig.1.4-a.

Bottles coming from the first arc are sterilized in node v^1 and are re-direct with a certain probability α to node v^2 where some is filled with lemon fruit juice and with probability $1-\alpha$ to node v^3 where some is filled with orange fruit juice. Assume that lemon and orange fruit juice bottles have two different shapes. In nodes v^4 and v^5, bottles are labeled as their own fruit juice. Finally in node v^6, produced bottles are corked. In this situation the dynamics at node v^1 is solved using the **RA1** algorithm. In fact, the redirection of bottles in order to maximize the production is not possible, since bottles have different shapes for any kind of juice.

Consider now a supply network as shown in Fig.1.4-b in which the white cups are addressed towards n arcs (or sub-chains) to be colored using different colors. Since the aim is to maximize the cups production independently from the colors, a mechanism is realized which addresses the cups on the outgoing sub-chains taking into account their loads in such way as to maximize flux on both incoming and

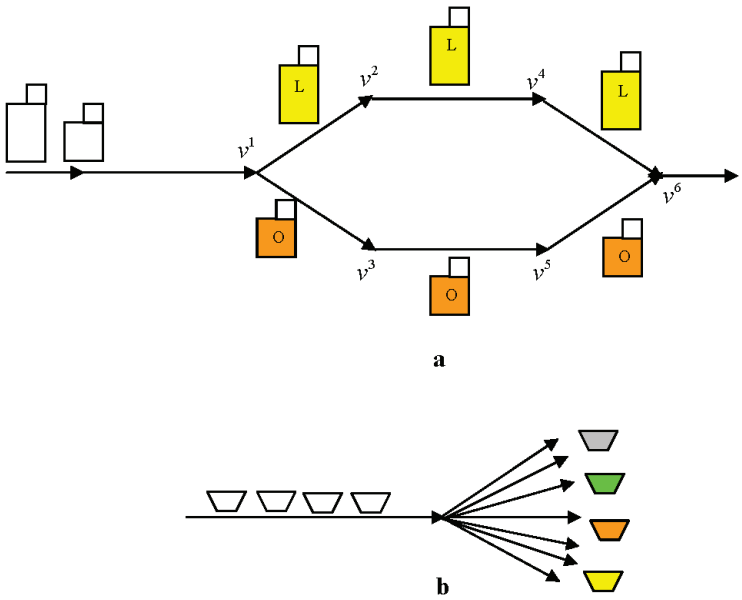

Figure 1.4: Supply network.

outgoing sub-chains. So, a model based on rule **RA2** is realized to capture the behavior of this network.

1.4.1 Basic Definitions

We start from the conservation law model

$$\rho_t + \left(\min\left\{\mu\left(t,x\right),\rho\right\}\right)_x = 0. \tag{1.45}$$

To avoid problems of existence of solutions, we assume μ piecewise constant and an evolution equation of semi-linear type:

$$\mu_t + \bar{V}\mu_x = 0, \tag{1.46}$$

where $\bar{V}$ is some constant velocity. Taking $\bar{V} = 0$, it can be no solution to a Riemann Problem for the system (1.45)-(1.46) with data (ρ_l, μ_l) and (ρ_r, μ_r) if $\min\{\rho_l, \mu_l\} > \mu_r$. Since we expect the chain to influence backward the processing rate we assume $\bar{V} < 0$ and for simplicity we set $\bar{V} = -1$.

A supply network consists of $N+1$ sub-chains $I_1, ..., I_{N+1}$, modeled by real intervals $\left[a^k, b^k\right] \subset \mathbb{R}$, $k = 1, ..., N+1$, $a_k < b_k$, possible with either $a_k = -\infty$ or

$b_k = +\infty$ and M suppliers or processors $P_1, ..., P_M$ with certain throughput times and capacity.

Each supplier processes a certain good, measured in units of parts. It is assumed that a node P consists of a processor, which decides how to manage the flow among sub-chains, with a maximal processing rate μ.

The evolution on each arc is given by (1.45)-(1.46), while at each nodes vertex the evolution is given by solving Riemann Problems for the density equation (1.45) with μs as parameters. Since such Riemann Problems may still admit no solution keeping the values of μs constant, then we expect μ waves to be generated following equation (1.46). Moreover the vanishing of the characteristic velocity for (1.45), in case $\rho > \mu$, can provoke resonances with the nodes (which can be presented schematically as waves with zero velocities). Then, for this reason, the model is modified as follows.

Each sub-chain I_k is characterized by a maximum density $\rho_k^{\max}$, a maximum processing rate $\mu_k^{\max}$ and a flux f_ε^k. Then the dynamics is given by:

$$\begin{cases} \rho_t + f_\varepsilon^k(\rho,\mu)_x = 0, \\ \mu_t - \mu_x = 0. \end{cases} \tag{1.47}$$

The flux is defined as:

$$\textbf{(F)}\quad f_\varepsilon^k(\rho,\mu) = \begin{cases} \rho, & 0 \le \rho \le \mu, \\ \mu + \varepsilon(\rho - \mu), & \mu \le \rho \le \rho_k^{\max}, \end{cases}$$

$$f_\varepsilon^k(\rho,\mu) = \begin{cases} \varepsilon\rho + (1-\varepsilon)\mu, & 0 \le \mu \le \rho, \\ \rho, & \rho \le \mu \le \mu_k^{\max}, \end{cases}$$

as shown in (Fig.1.5).

The conservation law for the good density in (1.47) is a ε perturbation of (1.45) in the sense that $||f - f\varepsilon||_\infty \le C\varepsilon$ where f is the flux of (1.47). The equation has the advantage of producing waves with always strictly positive speed, thus avoiding resonance with the "boundary" problems at each node.

From now on, fixing $\varepsilon > 0$ and dropping the indices, the flux will be indicated by $f(\rho,\mu)$.

Remark 7 *It is possible to generalize all following definitions and results to the case of different fluxes $f_{\varepsilon_k}^k$ for each sub-chain I_k (also choosing ε dependent on*

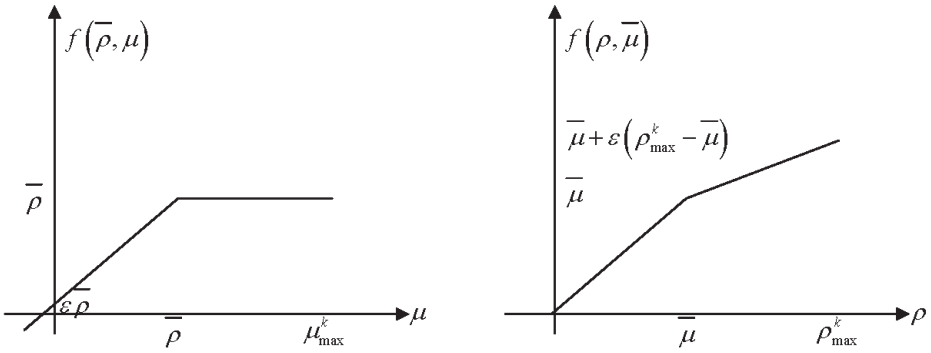

Figure 1.5: Flux (F): Left, $f(\bar{\rho},\mu)$. Right, $f(\rho,\bar{\mu})$.

k). In fact, all statements are in terms of values of fluxes at endpoints of the sub-chains, thus it is sufficient that the ranges of fluxes intersect. Moreover, we can consider different slopes m_k for each sub-chain I_k, considering the following flux

$$f^k_\varepsilon(\rho,\mu)=\begin{cases} m_k\rho, & 0\le\rho\le\mu,\\ m_k\mu+\varepsilon(\rho-\mu), & \mu\le\rho\le\rho^{\max}_k,\end{cases}$$

where $m_k\ge 0$ represents the velocity of each processor and is given by

$$m_k=\frac{L_k}{T_k},$$

with L_k and T_k, respectively, fixed length and processing time of processor k.

Assuming that the sub-chains are connected by some junction J, each of them is given by a finite number of incoming and outgoing sub-chains, then J is identified with $((i_1,...,i_n),(j_1,...,j_m))$ (see Fig.1.6) where the first n-tuple and the second m-tuple indicate respectively the set of incoming and outgoing sub-chains. Moreover, each sub-chain can be incoming or outgoing at most for one junction. Hence, the complete model is given by a couple (I,P), where $I=\{I_k : k=1,...,N+1\}$ is the collection of sub-chains and P is the collection of junctions.

The supply network evolution is described by a finite set of functions ρ_k, μ_k defined on $[0,+\infty[\times I_k$. On each sub-chain I_k, we say that $U_k:=(\rho_k,\mu_k):[0,+\infty[\times I_k\to\mathbb{R}$ is a weak solution to (1.47) if, for every C^∞-function $\varphi:[0,+\infty[\times I_k\to\mathbb{R}^2$ with compact support in $]0,+\infty[\times]a_k,b_k[$,

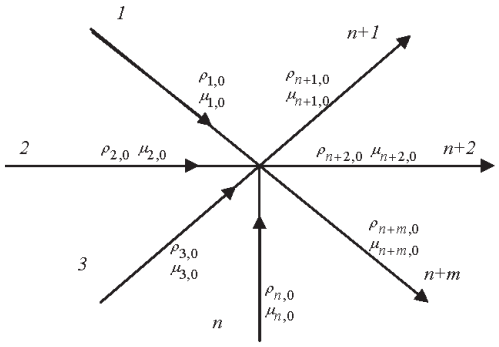

Figure 1.6: A junction.

$$\int_0^{+\infty} \int_{a_k}^{b_k} \left(U_k \frac{\partial \varphi}{\partial t} + f\left(U_k\right) \frac{\partial \varphi}{\partial x} \right) dxdt = 0,$$

where

$$f\left(U_k\right) = \begin{pmatrix} f\left(\rho_k, \mu_k\right) \\ -\mu_k \end{pmatrix},$$

is the flux function of the system (1.47). For definition of entropic solution, see at [7].

For a scalar conservation law, a Riemann Problem (RP) is a Cauchy problem for an initial data of Heavyside type, that is a piecewise constant with only one discontinuity. The solutions are formed by continuous waves called rarefactions and by traveling discontinuities called shocks.

Analogously, we call Riemann problem for a junction the Cauchy problem corresponding to an initial data which is constant on each supply sub-chain.

Definition 8 *A Riemann Solver (RS) for the junction P with n incoming sub-chains and m outgoing ones consists in a map that associates to a Riemann data $(\rho_0, \mu_0) = (\rho_{1,0}, \mu_{1,0}, ..., \rho_{n,0}, \mu_{n,0}, \rho_{n+1,0}, \mu_{n+1,0}, ..., \rho_{n+m,0}, \mu_{n+m,0})$ at P a vector $(\hat{\rho}_0, \hat{\mu}_0) = (\hat{\rho}_1, \hat{\mu}_1, ..., \hat{\rho}_n, \hat{\mu}_n, \hat{\rho}_{n+1}, \hat{\mu}_{n+1}, ..., \hat{\rho}_{n+m}, \hat{\mu}_{n+m})$ so that the solution is given by the waves $(\rho_{i,0}, \hat{\rho}_i)$ and $(\mu_{i,0}, \hat{\mu}_i)$ on the sub-chain I_i, $i = 1, ..., n$ and by the waves $(\hat{\rho}_j, \rho_{j,0})$ on the sub-chain I_j, $j = n+1, ..., n+m$. We require the consistency condition*

(CC) $RS\left(RS\left(\left(\rho_0,\mu_0\right)\right)\right)=RS\left(\left(\rho_0,\mu_0\right)\right).$

Once a Riemann Solver is assigned, we can define admissible solutions at P.

Definition 9 *Assume a Riemann Solver RS is assigned for the supplier P. Let $U=(U_1,...,U_{n+m})$ be such that U is of bounded variation for every $t\geq 0$. Then U is an admissible weak solution of (1.47) related to RS at the junction P if and only if the following property holds for almost every t. Setting*

$$\tilde{U}_p\left(t\right)=\left(U_1\left(\cdot,b_1-\right),...,U_n\left(\cdot,b_n-\right),U_{n+1}\left(\cdot,a_{n+1}+\right),...,U_{n+m}\left(\cdot,a_{n+m}+\right)\right)$$

we have $RS\left(\tilde{U}_p\left(t\right)\right)=\tilde{U}_p\left(t\right)$.

The aim is to solve the Cauchy problem on $[0,+\infty[$ for a given initial and boundary data as in next definition.

Definition 10 *Given $U_k:I_k\to[0,1]$, $k=1,...N+1$, measurable BV functions, a collection of functions $U=(U_1,...,U_{N+1})$, with $U_k:[0,+\infty[\times I_k\to[0,1]$ continuous as functions from $[0,+\infty[$ into L^1_{loc} and $U_k\left(t,\cdot\right)$ BV function for almost every t, is an admissible solution to the Cauchy problem on the supply chain if U_k is a weak entropic solution to (1.47) on I_k, $U_k\left(0,x\right)=\bar{U}_k\left(x\right)$ a.e., and, at each supplier P_k, U is an admissible weak solution.*

1.4.2 Riemann Solvers for suppliers

Fixing a sub-chain I_k, we analyze system (1.47) as a system of conservation laws in the variables $U=(\rho,\mu)$:

$$U_t+F\left(U\right)_x=0, \tag{1.48}$$

with flux function given by $F\left(U\right)=\left(f\left(\rho,\mu\right),-\mu\right)$, thus the Jacobian matrix of the flux is:

$$DF\left(\rho,\mu\right)=\begin{cases}\begin{pmatrix}1&0\\0&-1\end{pmatrix}, & \text{if } \rho<\mu,\\ \begin{pmatrix}\varepsilon&1-\varepsilon\\0&-1\end{pmatrix}, & \text{if } \rho>\mu.\end{cases}$$

The eigenvalues and eigenvectors are given by:

$$\lambda_1(\rho,\mu) \equiv -1, \qquad r_1(\rho,\mu) = \begin{cases} \begin{pmatrix} 0 \\ 1 \end{pmatrix}, & \text{if } \rho < \mu, \\ \begin{pmatrix} -\frac{1-\varepsilon}{1+\varepsilon} \\ 1 \end{pmatrix}, & \text{if } \rho > \mu, \end{cases}$$

$$\lambda_2(\rho,\mu) = \begin{cases} 1 & \text{if } \rho < \mu, \\ \varepsilon & \text{if } \rho > \mu, \end{cases} \qquad r_1(\rho,\mu) \equiv \begin{pmatrix} 0 \\ 1 \end{pmatrix}.$$

Hence the Hugoniot curves for the first family are vertical lines above the secant $\rho = \mu$ and lines with slope close to $-\frac{1}{2}$ below the same secant. The Hugoniot curves for the second family are just horizontal lines. Since we consider positive and bounded values for the variables, we fix the invariant region (see Fig.1.7):

$$D = \{(\rho,\mu) : 0 \le \rho \le \rho_{\max},\ 0 \le \mu \le \mu_{\max},$$
$$0 \le (1+\varepsilon)\rho + (1-\varepsilon)\mu \le (1+\varepsilon)\rho_{\max} = 2(1-\varepsilon)\mu_{\max}\}$$

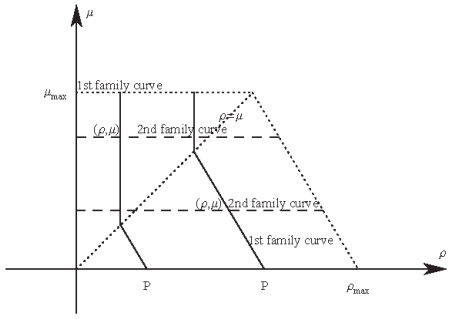

Figure 1.7: First and second family curves.

Observe that

$$\rho_{\max} = \mu_{\max}\frac{2}{1+\varepsilon}. \tag{1.49}$$

First, some results, widely proved for sequential supply chains in [14], are reported.

Proposition 11 *Given (ρ_0, μ_0), the minimal value of the flux at points of the curve of the first family passing through (ρ_0, μ_0) is given by:*

$$f_{\min}\left((\rho_0, \mu_0)\right) = \begin{cases} \frac{2\varepsilon}{1+\varepsilon}\rho_0, & if\ \rho_0 \leq \mu_0, \\ \varepsilon\rho_0 + \frac{\varepsilon(1-\varepsilon)}{1+\varepsilon}\mu_0, & if\ \rho_0 > \mu_0. \end{cases}$$

Lemma 12 *Given an initial datum (ρ_0, μ_0), the maximum value of the density of the curve of the second family passing through (ρ_0, μ_0) and belonging to the invariant region is given by*

$$\rho^M(\mu_0) = \rho_{\max} - \mu_0 \frac{\rho_{\max} - \mu_{\max}}{\mu_{\max}}. \tag{1.50}$$

Proof. From Fig.1.7 the maximum value is obtained by the intersection of the curve of the second family passing through (ρ_0, μ_0) and the line connecting the points $(\rho_{\max}, 0)$ and $(\mu_{\max}, \mu_{\max})$:

$$\rho^M(\mu_0) = \rho_{\max} - \mu_0 \frac{\rho_{\max} - \mu_{\max}}{\mu_{\max}}.$$

From (1.49) we get

$$\rho^M(\mu_0) = \frac{2}{1+\varepsilon}\mu_{\max} - \frac{(1-\varepsilon)}{1+\varepsilon}\mu_0.$$

■

The following estimate holds [14]:

Proposition 13 *Assume that a second family wave $((\rho_l, \mu_l), (\rho_m, \mu_m))$ interacts with a first family wave $((\rho_m, \mu_m), (\rho_r, \mu_r))$. If $\mu_r < \mu_m$ then the flux variation decreases.*

Considering now a node P with n and m respectively incoming and outgoing sub-chains and a Riemann initial datum $(\rho_{1,0}, \mu_{1,0}, ..., \rho_{n,0}, \mu_{n,0})$ and $(\rho_{n+1,0}, \mu_{n+1,0}, ..., \rho_{m+n,0}, \mu_{m+n,0})$, the following Lemma holds:

Lemma 14 *On the incoming sub-chain, only waves of the first family may be produced, while on the outgoing sub-chain only waves of the second family may be produced.*

From the last Lemma, assigned the initial datum, for each Riemann Solver it follows that

$$\begin{aligned} \hat{\rho}_i &= \varphi\left(\hat{\mu}_i\right), \quad i = 1, ..., n, \\ \hat{\mu}_j &= \mu_{j,0}, \qquad j = n+1, ..., n+m. \end{aligned} \tag{1.51}$$

where the function $\varphi(\cdot)$ describes the first family curve $(\rho_{i,0}, \mu_{i,0})$ as function of $\hat{\mu}_i$. The expression of such curve changes at a particular value $\bar{\mu}_i$, given by:

$$\bar{\mu}_i = \begin{cases} \rho_{i,0}, & if\ \rho_{i,0} \leq \mu_{i,0}, \\ \frac{1+\varepsilon}{2}\rho_{i,0} + \frac{1-\varepsilon}{2}\mu_{i,0}, & if\ \rho_{i,0} > \mu_{i,0}. \end{cases}$$

The case of sequential supply chain.

Considering a node P_k with one incoming arc k and one outgoing arc $k+1$. Let us now to discuss how $\hat{\rho}_{k+1}$ and $\hat{\mu}_k$ (from 1.51 we set $i = k$ and $j = k+1$) can be chosen.

The conservation of flux at the node can be written as

$$f\left(\varphi\left(\hat{\mu}_k\right), \hat{\mu}_k\right) = f\left(\hat{\rho}_{k+1}, \mu_{k+1,0}\right). \tag{1.52}$$

We have:

Case α): $\mu_{k+1,0} < \bar{\mu}_k$;

Case β): $\bar{\mu}_k \leq \mu_{k+1,0}$.

In both cases $\bar{\mu}_k$ and $\mu_{k+1,0}$ individuate in the plane $(\hat{\rho}_{k+1}, \hat{\mu}_k)$ four regions so defined:

$$\begin{aligned} A &= \left\{(\hat{\rho}_{k+1}, \hat{\mu}_k) : 0 \leq \hat{\rho}_{k+1} \leq \mu_{k+1,0}, \bar{\mu}_k \leq \hat{\mu}_k \leq \mu_k^{\max}\right\}; \\ B &= \left\{(\hat{\rho}_{k+1}, \hat{\mu}_k) : \mu_{k+1,0} \leq \hat{\rho}_{k+1} \leq \rho_{k+1}^M, \bar{\mu}_k \leq \hat{\mu}_k \leq \mu_k^{\max}\right\}; \\ A &= \left\{(\hat{\rho}_{k+1}, \hat{\mu}_k) : 0 \leq \hat{\rho}_{k+1} \leq \mu_{k+1,0}, 0 \leq \hat{\mu}_k \leq \bar{\mu}\right\}; \\ B &= \left\{(\hat{\rho}_{k+1}, \hat{\mu}_k) : \mu_{k+1,0} \leq \hat{\rho}_{k+1} \leq \rho_{k+1}^M, 0 \leq \hat{\mu}_k \leq \bar{\mu}_k\right\}; \end{aligned}$$

The (1.52) is satisfied in case β) along the line depicted in Fig.1.8 and in case α) (Fig.1.9) there are solutions, only under some conditions, along the dashed line. For details, see [14].

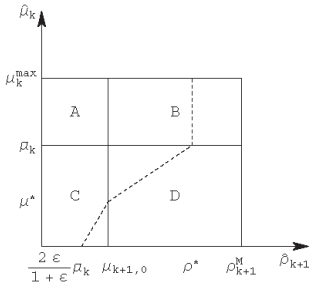

Figure 1.8: Case α).

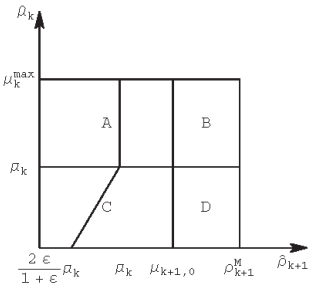

Figure 1.9: Case β).

A Riemann Solver according to rule SC1. Geometrically, in case β), we can define a Riemann Solver mapping every initial datum on the line $\hat{\mu}_k = c$ to the intersection of the same line with that drawn in Fig.1.9. While in case α), it may happen that there is no admissible solution on a given line $\hat{\mu}_k = c$. Therefore, we can use the same procedure if the line $\hat{\mu}_k = c$ intersects the dashed line of Fig.1.8, while mapping all other points to the admissible solution with the highest value of $\hat{\mu}_k$. This Riemann Solver is shown in Fig.1.10 and Fig.1.11.

Remark 15 *If $\hat{\rho}_{k+1} \leq \mu_{k+1,0}$, then the solution $(\hat{\rho}_{k+1}, \rho_{k+1,0})$ is a contact discontinuity. The same happens if $\hat{\rho}_{k+1} \geq \mu_{k+1,0}$ and $\rho_{k+1,0} > \mu_{k+1,0}$. If $\hat{\rho}_{k+1} \geq \mu_{k+1,0}$ and $\rho_{k+1,0} < \mu_{k+1,0}$, the solution consists of two discontinuities.*

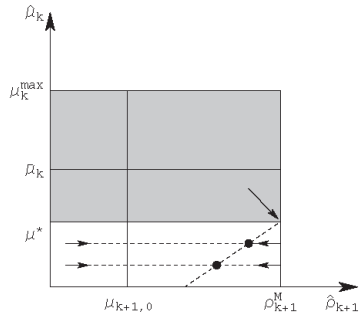

Figure 1.10: An example of Riemann Solver: case α.

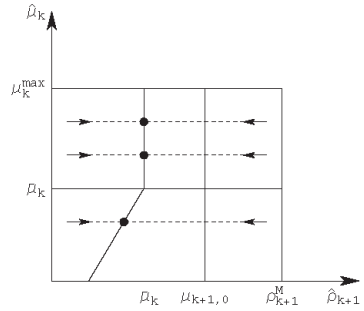

Figure 1.11: An example of Riemann Solver: case β.

A Riemann Solver according to rule SC2. Rule SC2 identifies a specific Riemann Solver:

Theorem 16 *Fix a node P_k. For every Riemann initial datum $(\rho_{k,0}, \mu_{k,0}, \rho_{k+1,0}, \mu_{k+1,0})$ at P_k there exists a unique vector $(\hat{\rho}_k, \hat{\mu}_k, \hat{\rho}_{k+1}, \hat{\mu}_{k+1})$ solution of the Riemann Problem according to rule **SC2**.*

Proof. Given the initial datum $(\rho_{k,0}, \mu_{k,0}, \rho_{k+1,0}, \mu_{k+1,0})$, it holds

$$\hat{\rho}_k = \varphi\left(\hat{\mu}_k\right),$$
$$\hat{\mu}_{k+1} = \mu_{k+1,0},$$

where $\varphi\left(\hat{\mu}_k\right)$ has been defined by (1.51). We have to distinguish again two cases:

Case α): $\mu_{k+1,0} < \bar{\mu}_k$. Let

$$\rho^* = \frac{\bar{\mu}_k - (1-\varepsilon)\,\mu_{k+1,0}}{\varepsilon}, \tag{1.53}$$

we consider two subcases which correspond to the situation in which solutions in region B exist or do not exist.

Case α_1): $\rho^* \leq \rho^M(\mu_{k+1,0})$. Since $\mu_{k+1,0} < \bar{\mu}_k$ we get

$$\rho^* = \frac{\bar{\mu}_k}{\varepsilon} - \left(\frac{1}{\varepsilon} - 1\right)\mu_{k+1,0} > \frac{\bar{\mu}_k}{\varepsilon} - \left(\frac{1}{\varepsilon} - 1\right)\bar{\mu}_k = \bar{\mu}_k.$$

Considering the lines of Fig.1.8, to every μ it corresponds a value of the flux. We claim the following:

Claim 17 *If $\rho^* \leq \rho^M$ the flux increases with respect to μ along the dashed lines in region C,D and in B for $\mu_k^{\max} \leq \mu \leq \rho^*$ and, finally, it is constant along the dashed line in region B for $\rho^* \leq \mu \leq \mu_k^{\max}$.*

It holds

$$f(\rho^*, \mu) = \begin{cases} \varepsilon\rho^* + (1+\varepsilon)\,\mu, & 0 \leq \mu \leq \rho^*, \\ \rho^*, & \rho^* \leq \mu \leq \mu_k^{\max}, \end{cases}$$

whose derivative, with respect to μ, is given by

$$\frac{\partial f(\rho^*, \mu)}{\partial \mu} = \begin{cases} (1+\varepsilon), & 0 \leq \mu \leq \rho^*, \\ 0, & \rho^* \leq \mu \leq \mu_k^{\max}. \end{cases}$$

It follows that for $\rho^* \leq \mu \leq \mu_k^{\max}$ the flux is constant along the dashed line in region B.

Let us now prove that the flux is increasing with respect to μ along the dashed lines in regions C and D. The line connecting the points $\left(\frac{2\varepsilon}{1+\varepsilon}\bar{\mu}_k, 0\right)$ and $(\mu_{k+1,0}, \mu^*)$ with $\mu^* = \frac{1+\varepsilon}{1-\varepsilon}\left(\hat{\mu}_{k+1} - \frac{2\varepsilon}{1+\varepsilon}\bar{\mu}_k\right)$ has equation

$$\rho - \frac{1}{\mu^*}\left(\mu_{k+1,0} - \frac{2\varepsilon}{1+\varepsilon}\bar{\mu}_k\right)\mu - \frac{2\varepsilon}{1+\varepsilon}\bar{\mu}_k = 0,$$

and a directional vector is given by

$$r_{C_\alpha} = \begin{pmatrix} \frac{1}{\mu^*}\left(\mu_{k+1,0} - \frac{2\varepsilon}{1+\varepsilon}\bar{\mu}_k\right) \\ 1 \end{pmatrix}.$$

Therefore, the directional derivative of the flux is equal to

$$\nabla f(\rho,\mu)\cdot r_{C_\alpha} = \begin{pmatrix} \varepsilon \\ 1-\varepsilon \end{pmatrix}\begin{pmatrix} \frac{1}{\mu^*}\left(\mu_{k+1,0} - \frac{2\varepsilon}{1+\varepsilon}\bar{\mu}_k\right) \\ 1 \end{pmatrix} = \\ = \frac{\varepsilon}{\mu^*}\left(\mu_{k+1,0} - \frac{2\varepsilon}{1+\varepsilon}\bar{\mu}_k\right) + (1-\varepsilon) > 0.$$

The latter inequality is fulfilled if $\mu_{k+1,0} > \frac{2\varepsilon}{1+\varepsilon}\bar{\mu}_k$, which is true whenever we have solutions in region C.

In region D a directional vector of the line connecting the points $(\mu_{k+1,0}, \mu^*)$ and $(\rho^*, \bar{\mu}_k)$ is the following

$$r_{D_\alpha} = \begin{pmatrix} \frac{\rho^* - \mu_{k+1,0}}{\bar{\mu}_k - \mu^*} \\ 1 \end{pmatrix}.$$

It implies that

$$\nabla f(\rho,\mu)\cdot r_{D_\alpha} = \begin{pmatrix} \varepsilon \\ 1-\varepsilon \end{pmatrix}\begin{pmatrix} \frac{\rho^* - \mu_{k+1,0}}{\bar{\mu}_k - \mu^*} \\ 1 \end{pmatrix} = \varepsilon\frac{\rho^* - \mu_{k+1,0}}{\bar{\mu}_k - \mu^*} + (1+\varepsilon) > 0,$$

since $\rho^* > \bar{\mu}_k > \mu_{k+1,0}$ and $\bar{\mu}_k - \mu^* > 0$.

In order to respect rule **SC2** we set

$$\rho_{k+1} = \rho^*, \\ \hat{\mu}_k = \min\left\{\mu_k^{\max}, \rho^*\right\}.$$

Case α_2): If $\rho^* > \rho^M(\mu_{k+1,0})$, there are not solutions in region B and since the flux increases with respect to μ in region D we set

$$\hat{\rho}_{k+1} = \rho^M, \\ \hat{\mu}_k = \tilde{\mu},$$

where $\tilde{\mu}$ is obtained from

$$(1-\varepsilon)\,\mu_{k+1,0} + \varepsilon\hat{\rho}_{k+1} = (1-\varepsilon)\,\hat{\mu}_k + \varepsilon\hat{\rho}_k,$$

setting $\hat{\rho}_{k+1} = \rho^M$, i.e.

$$\tilde{\mu} = \frac{\varepsilon(1+\varepsilon)}{1-\varepsilon}\rho^M - \frac{2\varepsilon}{1-\varepsilon}\bar{\mu}_k + (1+\varepsilon)\,\mu_{k+1,0} = \\ = \frac{2\varepsilon}{1-\varepsilon}\left(\mu_k^{\max} - \bar{\mu}_k\right) + \mu_{k+1,0}.$$

Case β): $\bar{\mu}_k \leq \mu_{k+1,0}$. Consider the line of Fig.1.9. In this case the flux is constant with respect to μ along the line in the region A and is an increasing function along the line in region C.

In fact, since the line in region A is given by $\hat{\rho}_{k+1} = \bar{\mu}_k$, it follows that

$$f\left(\hat{\rho}_{k+1}, \mu\right) = \begin{cases} \varepsilon\bar{\mu}_k + (1-\varepsilon)\,\mu, & 0 \leq \mu \leq \bar{\mu}_k, \\ \rho, & \bar{\mu}_k \leq \mu \leq \mu_k^{\max}, \end{cases}$$

from which

$$\frac{\partial f\left(\hat{\rho}_{k+1}, \mu\right)}{\partial \mu} = \begin{cases} (1-\varepsilon), & 0 \leq \mu \leq \bar{\mu}_k, \\ 0, & \bar{\mu}_k \leq \mu \leq \mu_k^{\max}. \end{cases}$$

In region C the line connecting the points $\left(\frac{2\varepsilon}{1-\varepsilon}\bar{\mu}_k, 0\right)$ and $(\bar{\mu}_k, \bar{\mu}_k)$ has equation

$$\rho - \frac{1-\varepsilon}{1+\varepsilon} - \frac{2\varepsilon}{1+\varepsilon}\bar{\mu}_k = 0,$$

and a directional vector is given by

$$r_{C_\beta} = \begin{pmatrix} \frac{1-\varepsilon}{1+\varepsilon} \\ 1 \end{pmatrix}.$$

The directional derivative is the following

$$\nabla f\left(\rho, \mu\right) \cdot r_{C_\beta} = \begin{pmatrix} \varepsilon \\ 1-\varepsilon \end{pmatrix} \begin{pmatrix} \frac{1-\varepsilon}{1+\varepsilon} \\ 1 \end{pmatrix} = \varepsilon\frac{1-\varepsilon}{1+\varepsilon} + (1-\varepsilon) > 0.$$

It follows that rule **SC2** is satisfied if we define

$$\begin{aligned} \hat{\rho}_{k+1} &= \bar{\mu}_k, \\ \hat{\mu}_k &= \bar{\mu}_k. \end{aligned}$$

Finally the Riemann Solver is the following:

Case α): $\mu_{k+1,0} < \bar{\mu}_k$

Case α_1): $\rho^* \leq \rho^M\left(\mu_{k+1,0}\right)$

$$\begin{aligned} \hat{\rho}_{k+1} &= \rho^*, \\ \hat{\mu}_k &= \min\left\{\mu_k^{\max}, \rho^*\right\}. \end{aligned}$$

Case α_2): $\rho^* > \rho^M(\mu_{k+1,0})$

$$\hat{\rho}_{k+1} = \rho^M(\mu_{k+1,0}),$$
$$\hat{\mu}_k = \tilde{\mu}.$$

Case β): $\mu_{k+1,0} \geq \bar{\mu}_k$

$$\hat{\rho}_{k+1} = \bar{\mu}_k,$$
$$\hat{\mu}_k = \bar{\mu}_k.$$

■

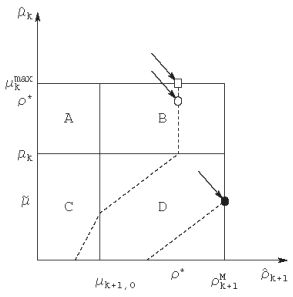

Figure 1.12: Case α) for the Riemann Solver **SC2**.

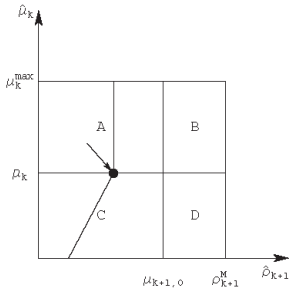

Figure 1.13: Case β) for the Riemann Solver **SC2**.

The Riemann Solver is shown in Fig.1.12 and Fig.1.13. In case α) we can define a Riemann Solver mapping every initial datum to the circle or to the square point if $\rho^* \leq \rho^M$ and to the filled point if $\rho^* > \rho^M$. In case β) we can define a Riemann Solver mapping every initial datum to the point $(\bar{\mu}_k, \bar{\mu}_k)$, indicated by the arrow.

A Riemann Solver according to rule SC3 Also with rule **SC3**, we have a precise Riemann Solver.

Theorem 18 *Fix a node P_k. For every Riemann initial datum $(\rho_{k,0}, \mu_{k,0}, \rho_{k+1,0}, \mu_{k+1,0})$ at P_k there exists a unique vector $(\hat{\rho}_k, \hat{\mu}_k, \hat{\rho}_{k+1}, \hat{\mu}_{k+1})$ solution of the Riemann Problem according to rule **SC3**.*

Proof. As for the Riemann Solver for rule **SC2**, given the initial datum $(\rho_{k,0}, \mu_{k,0}, \rho_{k+1,0}, \mu_{k+1,0})$, we have

$$\begin{aligned} \hat{\rho}_k &= \varphi\left(\hat{\mu}_k\right), \\ \hat{\mu}_{k+1} &= \mu_{k+1,0}, \end{aligned}$$

We distinguish:

Case α): This case is splitted in two subcases:

Case α_1): $\rho^* \leq \rho^M(\mu_{k+1,0})$. In theorem 64 it was proved that the flux increases with respect to μ along the dashed lines in regions C, D and B for $\mu_k^{\max} \leq \mu \leq \rho^*$ and, finally, it is constant along the line in region B for $\rho^* \leq \mu \leq \mu_k^{\max}$. It follows that we have to consider two situations:

Case α_{11}): $\rho^* > \mu_k^{\max}$. According to rule **SC3** we set

$$\begin{aligned} \hat{\rho}_{k+1} &= \rho^*, \\ \hat{\mu}_k &= \mu_k^{\max}. \end{aligned}$$

Case α_{12}): $\rho^* \leq \mu_k^{\max}$. We set

$$\begin{aligned} \hat{\rho}_{k+1} &= \rho^*, \\ \hat{\mu}_k &= \max\left\{\rho^*, \mu_{k+1}\right\}. \end{aligned}$$

Case α_2): $\rho^* > \rho^M(\mu_{k+1,0})$. In this case, there are not solutions in region B and since the flux increases with respect to μ in region D we set, as for the Riemann Solver **SC2**,

$$\begin{aligned} \hat{\rho}_{k+1} &= \rho^M\left(\mu_{k+1,0}\right), \\ \hat{\mu}_k &= \tilde{\mu}. \end{aligned}$$

Case β): The flux is constant with respect to μ along the line in the region A and is an increasing function along the line in region C, then we set

$$\hat{\rho}_{k+1} = \bar{\mu}_k,$$
$$\hat{\mu}_k = \begin{cases} \bar{\mu}_k, & \text{if } \mu_{k,0} < \bar{\mu}_k, \\ \mu_{k,0}, & \text{if } \mu_{k,0} \geq \bar{\mu}_k. \end{cases}$$

■

The obtained Riemann Solver is shown in Fig.1.14: all points of the white region are mapped horizontally and all points of the dark regions are mapped to the point indicated by the arrows.

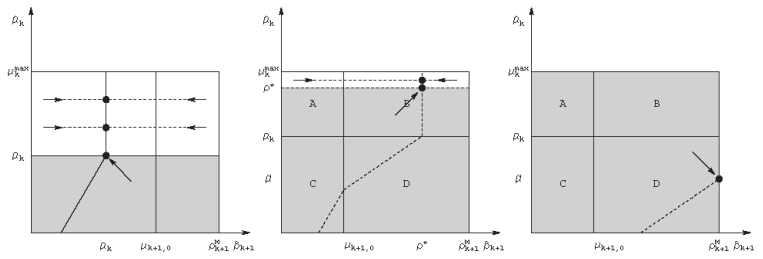

Figure 1.14: Case β) and α) (namely α_1) and α_2)) for the Riemann Solver **SC3**.

Analogously to the case of rule **SC1**, we can give conditions for solvability of Riemann Problems, more precisely:

Lemma 19 *Consider a supply chain on which the initial datum verifies $\mu_{k,0} = \mu_k^{\max}$, i.e. the production rate is at its maximum. A sufficient condition for the solvability of all Riemann Problems, according to rule **SC2** or **SC3**, on the supply chain at every time is*

$$\rho_{k+2}^{\max} \geq \rho_k^{\max}, \ \forall k.$$

The case of a supply chain networks

Now, two different Riemann Solvers at junction are defined according to the routing algorithms **RA1** and **RA2**. For both these algorithms, the flux of goods can be maximized considering the two additional rules **SC2** and **SC3**.

In order to define Riemann problems according to **RA1** and **RA2** let us introduce the notation:

$$f_k = f\left(\rho_k, \mu_k\right).$$

The maximum flux obtainable by a wave solution on each production sub-chain:

$$f_k^{\max} = \begin{cases} \bar{\mu}_k, & k = 1, ..., n, \\ \mu_{k,0} + \varepsilon\left(\rho^M\left(\mu_{k,0}\right) - \mu_{k,0}\right), & k = n+1, ..., n+m. \end{cases}$$

Since $\hat{f}_i \in \left[f_i^{\min}, f_i^{\max} = \bar{\mu}_i\right]$, $i = 1, ..., n$ and $\hat{f}_j \in \left[0, f_j^{\max} = \mu_{j,0} + \varepsilon\left(\rho^M\left(\mu_{j,0}\right) - \mu_{j,0}\right)\right]$, $j = n+1, ..., n+m$ it follows that if

$$\sum_{i=1}^{n} f_i^{\max} > \sum_{j=n+1}^{n+m} f_j^{\max}$$

the Riemann Problem does not admit solution. For the solvability of the supply network the following conditions hold:

Lemma 20 *A necessary and sufficient condition for the solvability of the Riemann Problem is that*

$$\sum_{i=1}^{n} f_i^{\max} \leq \sum_{j=n+1}^{n+m} \mu_{j,0} + \varepsilon\left(\rho^M\left(\mu_{j,0}\right) - \mu_{j,0}\right).$$

Lemma 21 *A sufficient condition for the solvability of the Riemann Problems, independent of the initial data, is the following*

$$\sum_{i=1}^{n} \rho_i^{\max} \leq \sum_{j=n+1}^{n+m} \mu_j^{\max}.$$

Proof. Since $\hat{f}_i \in \left[f_i^{\min}, f_i^{\max}\right]$, $i = 1, ..., n$ and $\hat{f}_j \in \left[0, f_j^{\max}\right]$, $j = n+1, ..., n+m$, the worst case to fulfill the condition of Lemma XX(prec) happens when $f_i^{\min}$ assumes the greatest value and $f_j^{\max}$ the lowest one

$$\sum_{i=1}^{n} \varepsilon \rho_i^{\max} \leq \varepsilon \sum_{j=n+1}^{n+m} \mu_j^{\max}.$$

■

Now, considering a single junction P, we analyze two cases:

1. P with $n-1$ incoming arcs and 1 outgoing arc (i.e. $(n-1) \times 1$ node);
2. P with 1 incoming arc and $m-1$ outgoing arcs (i.e. $1 \times (m-1)$ node).

One outgoing sub-chain

In this case, since there is only one outgoing sub-chain, the algorithms **RA1** and **RA2** coincide.

Fixing a Riemann initial datum $(\rho_0, \mu_0) = (\rho_{1,0}, \mu_{1,0}, ..., \rho_{n-1,0}, \mu_{n-1,0}, \rho_{n,0}, \mu_{n,0})$, let us denote the solution of the Riemann Problem with $(\hat{\rho}, \hat{\mu}) = (\hat{\rho}_1, \hat{\mu}_1, ..., \hat{\rho}_{n-1}, \hat{\mu}_{n-1}, \hat{\rho}_n, \hat{\mu}_n)$ and introduce the priority parameters $(q_1, q_2, ..., q_{n-1})$ which determine a *level of priority* at the junction sub-chains (see Fig.1.15).

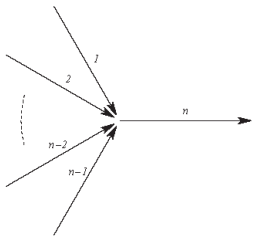

Figure 1.15: One outgoing sub-chain.

Let us define

$$\Gamma_{inc} = \sum_{i=1}^{n-1} f_i^{\max},$$
$$\Gamma_{out} = f_n^{\max},$$

and $\Gamma = \min\{\Gamma_{inc}, \Gamma_{out}\}$.

For simplicity, we analyze a junction with $n = 3$, so we need only one priority parameter $q \in]0, 1[$. Think, for example, of a filling station for soda cans. The sub-chain 3 fills the cans, whereas sub-chains 1 and 2 produce plastic and aluminium cans, respectively.

First, we compute $\hat{f}_i$ $i = 1, 2, 3$ and then $\hat{\rho}_i$ and $\hat{\mu}_i$, $i = 1, 2, 3$.

We have to distinguish two cases:

Case 1): $\Gamma = \Gamma_{inc}$.

Case 2): $\Gamma < \Gamma_{inc}$.

In the first case we set $\hat{f}_i = f_i^{\max}$, $i = 1, 2$.

Instead, in the second case we have to use the priority parameter q. Since not all objects can enters the junction, letting C be the amount of objects that can go through, then qC and $(1-q)\,C$ are the objects coming respectively from first and second sub-chain.

Considering the space (f_1, f_2), we define the following line:

$$r_q : f_2 = \frac{1-q}{q} f_1,$$
$$r_\Gamma : f_1 + f_2 = \Gamma.$$

Define P to be the point of intersection of the lines r_q and r_Γ. Recall that the final fluxes should belong to the region (as in Fig.1.16):

$$\Omega = \{(f_1, f_2) : 0 \leq f_i \leq f_i^{\max}, i = 1, 2\}.$$

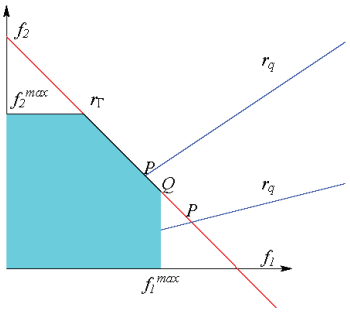

Figure 1.16: P belongs to Ω and P is outside Ω.

We distinguish two cases:

a) P belongs to Ω,

b) P is outside Ω.

In the first case we set $\left(\hat{f}_1, \hat{f}_2\right) = P$, while in the second case we set $\left(\hat{f}_1, \hat{f}_2\right) = Q$, with $Q = proj_{\Omega \cap r_\Gamma}(P)$ where $proj$ is the usual projection on a convex set (Fig.1.16). Notice that $\hat{f}_3 = \Gamma$.

Remark 22 *The same reasoning can be done also in the case of $n-1$ incoming sub-chains. In $\mathbb{R}^{n-1}$ we get the line $r_q = tv_q$, $t \in \mathbb{R}$, with $v_q \in \Delta_{n-2}$ where*

$$\Delta_{n-2} = \left\{ (f_1, ..., f_{n-1}) : f_i \geq 0, i = 1, ..., n-1, \sum_{i=1}^{n-1} f_i = 1 \right\}$$

is the $(n-2)$ dimensional simplex and

$$H_\Gamma = \left\{ (f_1, ..., f_{n-1}) : \sum_{i=1}^{n-1} f_i = 1 \right\}$$

is a hyperplane. Since $v_q \in \Delta_{n-2}$, there exists an unique point $P = r_q \cap H_\Gamma$. If $P \in \Omega$, then we set $\left(\hat{f}_1, ..., \hat{f}_{n-1}\right) = P$. If $P \notin \Omega$, then we set $\left(\hat{f}_1, ..., \hat{f}_{n-1}\right) = Q = proj_{\Omega \cap r_\Gamma}(P)$, the projection over the subset $\Omega \cap H_\Gamma$. Observe that the projection is unique since $\Omega \cap H_\Gamma$ is a closed convex subset of H_Γ.

In order to compute $\hat{\rho}_i$ and $\hat{\mu}_i$, $i = 1, 2, 3$, on the incoming sub-chains we have to distinguish two subcases:

Case 2.1): $\hat{f}_i = f_i^{\max}$. We set according to rules $SC2$ and $SC3$,

$$\begin{array}{lll} SC2: & \begin{array}{l} \hat{\rho}_i = \bar{\mu}_i, \\ \hat{\mu}_i = \bar{\mu}_i, \end{array} & i = 1, 2, \\ SC3: & \begin{array}{l} \hat{\rho}_i = \bar{\mu}_i, \\ \hat{\mu}_i = \max\left\{\bar{\mu}_i, \mu_{i,0}\right\}, \end{array} & i = 1, 2. \end{array}$$

In this case $\hat{\rho}_i = \varphi(\hat{\mu}_i) = \bar{\mu}_i$, $i = 1, 2$.

Case 2.2): $\hat{f}_i < f_i^{\max}$. There exists an unique $\hat{\mu}_i$ such that $\hat{\mu}_i + \varepsilon(\varphi(\hat{\mu}_i) - \hat{\mu}_i) = \hat{f}_i$. According to (1.51), we set $\hat{\rho}_i = \varphi(\hat{\mu}_i)$, $i = 1, 2$.

On the outgoing sub-chain we have:

$$\hat{\mu}_3 = \mu_{3,0},$$

while $\hat{\rho}_3$ is the unique value such that $f_\varepsilon(\mu_{3,0}, \hat{\rho}_3) = \hat{f}_3$.

One incoming sub-chain

Fixing a node P with 1 incoming arc and $m-1$ outgoing ones (see Fig.1.17), and a Riemann initial datum $(\rho_0, \mu_0) = (\rho_{1,0}, \mu_{1,0}, \rho_{2,0}, \mu_{2,0}, ..., \rho_{m,0}, \mu_{m,0})$, let us denote the solution of the Riemann Problem $(\hat{\rho}, \hat{\mu}) = (\hat{\rho}_1, \hat{\mu}_1, \hat{\rho}_2, \hat{\mu}_2, ..., \hat{\rho}_m, \hat{\mu}_m)$. For this configuration, we need to define the distribution of goods from the incoming arc. Then, we introduce the flux distribution parameters α_j, $j = 2, ..., m$, where

$$0 < \alpha_j < 1, \ \sum_{j=2}^{m} \alpha_j = 1.$$

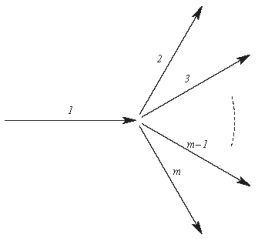

Figure 1.17: One incoming sub-chain.

The coefficient α_j represents the percentage of objects addressed from the arc 1 to the sub-chain j. The flux on the arc j is thus given by

$$f_j = \alpha_j f_1, \ j = 2, ..., m,$$

where f_1 is the incoming flux on the arc 1.

Let us define

$$\Gamma_{inc} = f_1^{\max},$$
$$\Gamma_{out} = \sum_{j=2}^{m} f_j^{\max},$$

and $\Gamma = \min\{\Gamma_{inc}, \Gamma_{out}\}$.

We have to determine $\hat{\mu}_k$ and $\hat{\rho}_k$, $k = 1, ..., m$, for both algorithms **RA1** and **RA2**.

Riemann solver according to RA1 Analyze the general case with m sub-chains. For example, we refer to the filling station for orange and lemon fruit juice bottles as shown in Fig.1.4-a, where the dynamics at node v^1 is solved using the algorithm we are going to describe.

Since $f_j \leq f_j^{\max}$ it follows that

$$f_1 \leq \frac{f_j^{\max}}{\alpha_j},\ j = 2, ..., m.$$

We set

$$\begin{aligned} &\hat{f}_1 = \min\left\{f_1^{\max}, \tfrac{f_j^{\max}}{\alpha_j}\right\}, \\ &\hat{f}_j = \alpha_j \hat{f}_1, \end{aligned} \qquad j = 2, ..., m.$$

On the incoming sub-chain we have to distinguish two subcases:

Case 1): $\hat{f}_1 = f_1^{\max}$. According to rule **SC2** and **SC3**, respectively, we set:

$$\begin{aligned} SC2: &\quad \hat{\rho}_1 = \bar{\mu}_1, \\ &\quad \hat{\mu}_1 = \bar{\mu}_1, \\ SC3: &\quad \hat{\rho}_1 = \bar{\mu}_1, \\ &\quad \hat{\mu}_1 = \max\left\{\bar{\mu}_1, \mu_{1,0}\right\}. \end{aligned}$$

Case 2): $\hat{f}_1 < f_1^{\max}$. In this case there exists an unique $\hat{\mu}_1$ such that $\hat{\mu}_1 + \varepsilon\left(\varphi\left(\hat{\mu}_1\right) - \hat{\mu}_1\right) = \hat{f}_1$. According to (1.51), we set $\hat{\rho}_1 = \varphi\left(\hat{\mu}_1\right)$.

On the outgoing sub-chain we have:

$$\hat{\mu}_j = \mu_{j,0},\ j = 2, 3, .., m$$

while $\hat{\rho}_i$ is the unique value such that $f_\varepsilon\left(\mu_{j,0}, \hat{\rho}_j\right) = \hat{f}_j$, $j = 2, 3, .., m$.

Riemann solver according to RA2 For simplicity let us consider a node with $m = 3$ and in this case we need only one distribution parameter $\alpha \in]0, 1[$ (referred to the cups production as shown in Fig.1.4-b). The dynamics at the node is solved according to the algorithm **RA2**. Compute $\hat{f}_k$, $k = 1, 2, 3$.

We have to distinguish two cases:

Case 1): $\Gamma = \Gamma_{out}$.

Case 2): $\Gamma < \Gamma_{out}$.

In the first case we set $\hat{f}_j = f_j^{\max}$, $j = 2, 3$, while in the second one we use the priority parameter α.

Then, if we indicate with C the amount of objects that can go through the junction, let αC and $(1-\alpha)\, C$ be the objects that respectively coming from the first and second sub-chain. Considering the space (f_2, f_3), define the following lines:

$$r_\alpha : f_3 = \tfrac{1-\alpha}{\alpha} f_2,$$
$$r_\Gamma : f_2 + f_3 = \Gamma.$$

Define P to be the point of intersection of the lines r_α and r_Γ. Recall that the final fluxes should belong to the region:

$$\Omega = \left\{ (f_2, f_3) : 0 \leq f_j \leq f_j^{\max},\ j = 2, 3 \right\}.$$

We distinguish two cases:

a) P belongs to Ω,

b) P is outside Ω.

In the first case we set $\left(\hat{f}_2, \hat{f}_3\right) = P$, while in the second case we set $\left(\hat{f}_2, \hat{f}_3\right) = Q$, with $Q = proj_{\Omega \cap r_\Gamma}(P)$ where $proj$ is the usual projection on a convex set. Notice that $\hat{f}_1 = \Gamma$.

Again, we can extend the reasoning to the case of $m-1$ outgoing sub-chains as for the incoming ones defining the hyperplane

$$H_\Gamma = \left\{ (f_2, ..., f_m) : \sum_{j=2}^{m} f_j = \Gamma \right\}$$

and choosing a vector $v_\alpha \in \Delta_{m-2}$. Moreover, we compute $\hat{\rho}_k$ and $\hat{\mu}_k$ in the same way described for the Riemann Solver **RA1**.

Remark 23 *In alternative, assuming that a traffic distribution matrix A is assigned, then we can compute $\hat{f}_1$ and choose the vector $v_\alpha \in \Delta_{m-2}$ by*

$$v_\alpha = \Delta_{m-2} \cap \left\{ tA\left(\hat{f}_1\right) : t \in \mathbb{R} \right\}.$$

Remark 24 *The classical Kruzkov entropy inequalities at nodes [7] read*

$$\sum_{inc} sgn\left(\rho - k\right)\left(f\left(\rho\right) - f\left(k\right)\right) \geq \sum_{out} sgn\left(\rho - k\right)\left(f\left(\rho\right) - f\left(k\right)\right)$$

over the sums are respectively over incoming and outgoing sub-chains and k is arbitrary. The fluxes are always monotone with respect to ρ, while the precise values taken by fluxes and densities on the sub-chains may be different. Thus we can not expect the inequality to hold in general.

1.4.3 Waves production

In this section let us discuss the waves production on an incoming and an outgoing sub-chain with initial datum $(\rho_{i,0}, \mu_{i,0})$ and $(\rho_{j,0}, \mu_{j,0})$ respectively.

Since the load dynamic is described by a conservation law in ρ and an evolution equation in μ, we have ρ-waves and μ-waves of two types:

- shocks waves which are discontinuities in ρ and/or μ traveling at a constant speed,
- contact discontinuities, which separate two constant states with the same speed but different values.

The last one are contact discontinuities in ρ and μ with speed $\lambda = -1$ connecting the states $\rho_{i,0}$ and $\hat{\rho}_i$ and $\mu_{i,0}$ and $\hat{\mu}_i$.

On the outgoing sub-chain only ρ-waves of the second family can be produced. Then we must consider two cases:

Case a): $\rho_{j,0} \leq \mu_{j,0}$.

Case b): $\rho_{j,0} > \mu_{j,0}$.

For the case a), two subcases have to be distinguished:

Case a.1): If $\hat{\rho}_j \in [0, \mu_{j,0}]$ then the solution of the Riemann Problem consists of a contact discontinuity connecting $\hat{\rho}_j$ and $\rho_{i,0}$ with speed 1 (for $t = 1$);

Case a.2): If $\hat{\rho}_j \in \left]\mu_{j,0}, \mu_j^{\max}\right]$ then the solution of the Riemann Problem consists of two shocks: one connecting $\hat{\rho}_j$ and $\mu_{j,0}$ with speed ε (for $t = 1$) followed

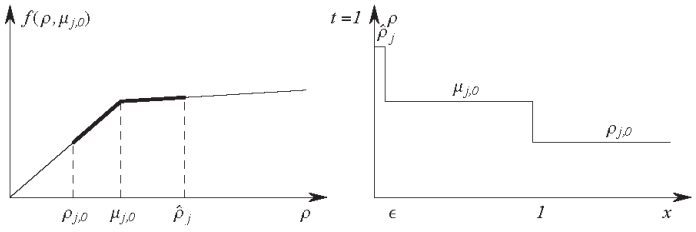

Figure 1.18: Waves production on an outgoing sub-chain: case a.2).

by another one connecting $\mu_{j,0}$ and $\rho_{j,0}$ traveling with speed 1 (for $t = 1$) (see Fig.1.18).

In the case b) we have to consider two subcases:

Case b.1): If $\hat{\rho}_j \in [0, \mu_{j,0}]$ then the solution of the Riemann Problem consists of a shock wave connecting the states $\hat{\rho}_j$ and $\rho_{j,0}$ with speed (for $t = 1$) equal to slope λ of the line connecting the two states:

$$\lambda = \frac{\mu_{j,0} + \varepsilon\left(\rho_{j,0} - \mu_{j,0}\right) - \hat{\rho}_j}{\rho_{j,0} - \hat{\rho}_j}.$$

Case b.2): If $\hat{\rho}_j \in \left]\mu_{j,0}, \mu_j^{\max}\right]$ then the solution of the Riemann Problem consists of a contact discontinuity connecting $\hat{\rho}_j$ and $\rho_{j,0}$ with speed ε (for $t = 1$).

1.5 Equilibrium analysis

Fixing a node P and a Riemann initial datum (ρ_0, μ_0), now we introduce some notions about the equilibria at nodes.

Definition 25 *Define* $(\hat{\rho}, \hat{\mu}) = RS\left((\rho_0, \mu_0)\right)$. *The datum* (ρ_0, μ_0) *is an equilibrium if*

$$(\hat{\rho}, \hat{\mu}) = RS\left((\rho_0, \mu_0)\right) = (\rho_0, \mu_0)\,.$$

Distinguishing two types of nodes, $(n-1) \times 1$ and $1 \times (m-1)$, and equilibria with active and not active constraints for the maximization problem, we consider generic equilibria for the Riemann Problem at a junction.

1.5.1 A node with one outgoing sub-chain

If the n-th sub-chain is an active constraint then we have:

$$\rho_n = \rho^M(\mu_n),$$

otherwise, if it is not an active constraint, we have:

$$\rho_n < \rho^M(\mu_n).$$

For the incoming sub-chains I_i, $i = 1, ..., n-1$, it will be: if the i-th sub-chain is an active constraint then

$$\begin{array}{ll} SC2: & \mu_i = \rho_i \\ SC3: & \mu_i \geq \rho_i \end{array}, \ i = 1, ..., n-1,$$

otherwise

$$\rho_i \geq \mu_i.$$

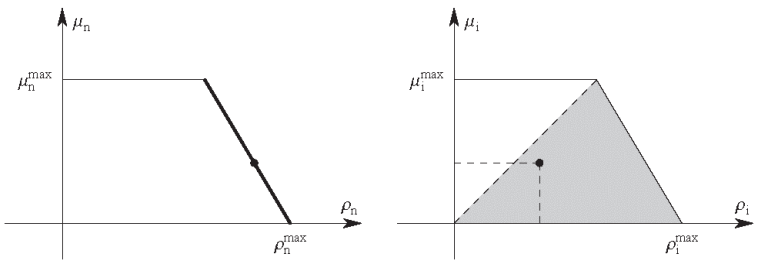

Figure 1.19: The outgoing sub-chain is an active constraint and the incoming ones are not active constraints.

In Fig.1.19 and Fig.1.20 the equilibria are shown. In the latter the equilibria for the algorithm **SC2** are depicted in bold, while for **SC3** in bold and grey.

The first type of equilibria (Fig.1.19) represents the situation in which the outgoing sub-chain exhibit the maximal production effort, while the incoming ones adjust accordingly their production flows.

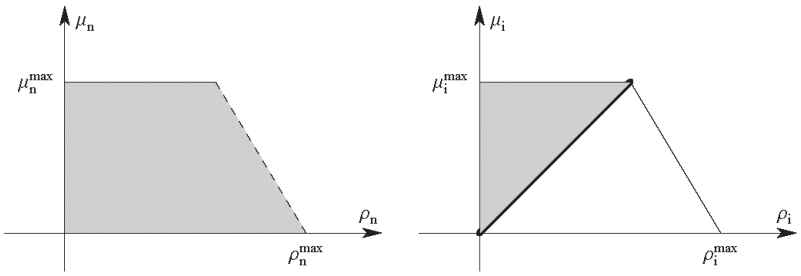

Figure 1.20: The incoming sub-chains are active constraints and the outgoing one is not an active constraint.

The second type (Fig.1.20) shows the situation in which the incoming sub-chains have a low level of part densities and, consequently, the outgoing sub-chain is not used at maximal level. In this case, then, since the whole plant is not used suitably, a re-building is in order, in fact it can be considered either the incoming sub-chains should be powered such that the production rate is improved or the outgoing ones should be restricted such that the production costs would be lower.

1.5.2 A node with one incoming sub-chain

The equilibria for the two algorithms **RA1** and **RA2** coincide. In particular, if the incoming sub-chain is an active constraint then

$$\begin{aligned} SC2: &\quad \rho_1 = \mu_1, \\ SC3: &\quad \rho_1 \leq \mu_1, \end{aligned}$$

otherwise $\rho_1 \geq \mu_1$.

Considering the outgoing sub-chains I_j, $j = 2, ..., m$, if I_j is an active constraint then $\rho_j = \rho^M(\mu_j)$ for both **SC2** and **SC3** algorithms, otherwise $\rho_j < \rho^M(\mu_j)$.

For both algorithms **RA1** and **RA2**, the case of incoming sub-chain as active constraint should happen only with $\rho_1 = \mu_1$, in such a way that the goods fill up appropriately the sub-chain. Otherwise the incoming sub-chain should be powered. For the outgoing sub-chains as active constraints, the situation is different. In fact, the latter represents a projecting error for the algorithm **RA1**, while it may well happen for **RA2**.

1.5.3 Bullwhip effect

The Bullwhip effect is a well known oscillation phenomenon in supply chain theory, see [12]. Since this effect consists in oscillations moving backwards, the most interesting case consists of nodes with $n-1$ incoming sub-chains and one outgoing sub-chain.

Then, to study the Bullwhip effect, we have to compute the oscillations on incoming sub-chains produced by the interaction with the node of a wave from the outgoing one. Since the wave must have negative speed, it is a first family wave. Fixing the notation, we denote with $-$ and $+$ the values before and after the interaction, and with Δ the jump in the values from the left to the right along waves traveling on sub-chains. Let (ρ^-, μ^-) be an equilibrium configuration at the node and $\left((\rho_n^-, \mu_n^-), (\tilde{\rho}_n, \tilde{\mu}_n)\right)$ the wave coming to the same node.

The effect of the interaction of the wave is the production of $n-1$ waves on the incoming sub-chains.

The oscillation amplitude in the production rate before the interaction is given by:

$$\Delta\mu^- = \tilde{\mu}_n - \mu_n^-.$$

The maximum flux on the outgoing sub-chain as function of μ is the following

$$f_n^{\max}(\mu) = \mu\frac{1-\varepsilon}{1+\varepsilon} + \varepsilon\rho_n^{\max},$$

thus it is an increasing function. The oscillation of the flux after the interaction is

$$\Delta f^+ = \frac{1-\varepsilon}{1+\varepsilon}\Delta\mu^-.$$

Now, assuming first that the incoming sub-chains are not active constraints, for both algorithms **SC2** and **SC3**, we have $\rho_i^- \geq \mu_i^-$, $i = 1, ..., n-1$. Then the first family curve passing through $\left(\rho_i^-, \mu_i^-\right)$, belonging to the region $\rho \geq \mu$, is given by

$$\rho = \rho_i^- + \left(\mu - \mu_i^-\right)\left(-\frac{1-\varepsilon}{1+\varepsilon}\right).$$

From which, for small oscillations we obtain

$$\Delta\rho^+ = -\frac{1-\varepsilon}{1+\varepsilon}\Delta\mu^+.$$

If the oscillation is not small the same relation holds with an inequality sign. Observe that

$$\Delta f^+ = \Delta\mu^+(1-\varepsilon) + \varepsilon\Delta\rho^+ = \frac{1-\varepsilon}{1+\varepsilon}\Delta\mu^+,$$

from which

$$\Delta\mu^+ = \frac{1+\varepsilon}{1-\varepsilon}\Delta f^+,$$

and then

$$\Delta\mu^+ = \Delta\mu^-.$$

Assume now that the incoming sub-chains are active constraints, which means that $\mu_i^- = \rho_i^-$ and $\mu_i^- = \rho_i^-$ respectively for **SC2** and **SC3** algorithm. Along the curve of the first family belonging to the region $\rho \leq \mu$ we have $\Delta f = 0$, i.e. a dumping effect is possible, while in the region $\rho \geq \mu$ we have

$$\Delta f = \frac{1-\varepsilon}{1+\varepsilon}\Delta\mu.$$

Considering the **SC2** algorithm, if the first family wave from the outgoing road increases the flux, then it is reflected as a second family wave. In the opposite case, we get the same estimates as above.

Considering the **SC3** algorithm, if the first family wave from the outgoing road increases the flux, then it is again reflected as a second family wave. In the opposite case, we get:

$$\Delta\mu^+ = \Delta\mu^- + \left(\mu_i^- - \rho_i^-\right)$$

with an increase in the production rate oscillation.

In conclusion we get the following:

Proposition 26 *The algorithm **SC3** may produce the Bullwhip effect. On the contrary, the algorithm **SC2** conserves oscillations or produce a dumping effect, thus not permitting the Bullwhip effect.*

Chapter 2

Numerical Schemes

In this chapter we present the numerical schemes for the Göttlich-Herty-Klar model and the continuum-discrete model for supply chains.

2.1 Numerical methods for Göttlich-Herty-Klar model

Considering the system (1.34)-(1.37), we want to obtain numerical results for parts dynamics inside a supply chain finding, for each arc j, a suitable approximation for the density $\rho_j(x,t)$ and the queue $q_j(t)$, with $0 \leq x \leq L_j$ and $t \in [0,T]$. In particular, we use the upwind scheme for densities (i.e referred to *PDE* of the model) and the explicit Euler scheme for queues (i.e referred to *ODE of the model*).

For each arc $j \in J$, define e numerical grid in $[0, L_j] \times [0,T]$ using the following notations:

- $\Delta x_j = \frac{L_j}{N_j}$ is the space grid size, where N_j is the number of segments into which we divide L_j (the length of j-th supplier);
- $\Delta t_j = \frac{T}{\eta_j}$ is the time grid size, where η_j is the number of segments into which we divide the interval $[0,T]$;
- $(x_i, t^n) = (i\Delta x_j, n\Delta t_j)$, $i = 0, ..., N_j$, $n = 0, ..., \eta_j$ are the grid points.

For the density function ρ_j defined on the grid, we set ${}^j\rho_i^n$ as the approximation of $\rho_j(x_i, t^n)$,with $j \in J$, $i = 0, ..., N_j$, $n = 0, ..., \eta_j$. For the queue q_j, q_j^n is the approximation of $q_j(t^n)$.

Without loss of generality, we can assume that for each arc j, $\Delta x_j = \Delta x$ and $\Delta t_j = \Delta t$, with Δx and Δt fixed.

A numerical scheme to solve conservation laws at each arc is the upwind method:

$$ {}^j\rho_i^{n+1} = {}^j\rho_i^n - \frac{\Delta t}{\Delta x}\frac{L_j}{T_j}\left({}^j\rho_i^n - {}^j\rho_{i-1}^n\right),\ j \in J,\ i = 0, ..., N_j,\ n = 0, ..., \eta_j. \tag{2.1} $$

The evolution of queues is described by the explicit Euler method:

$$ q_j^{n+1} = q_j^n + \Delta t\left(f_{j-1,out}^n - f_{j,inc}^n\right),\ j \in J - \{1\},\ n = 0, ..., \eta_j, \tag{2.2} $$

where $f_{j-1,out}^n$ and $f_{j,inc}^n$ are the approximation of $f_{j-1}\left(\rho_{j-1}\left(b_{j-1}, t^n\right)\right)$ and $f_j\left(\rho_j\left(a_j, t^n\right)\right)$, respectively, both depending on values of densities computed by (2.1).

In order to consider boundary data, we refer to equation (2.1) for $i = 0$. We proceed by inserting a ghost cell and defining

$$ {}^j\rho_0^{n+1} = {}^j\rho_0^n - \frac{\Delta t}{\Delta x}\frac{L_j}{T_j}\left({}^j\rho_0^n - {}^j u_0^n\right),\ j \in J,\ n = 0, ..., \eta_j, $$

where ${}^j u_0^n$ takes the place of ${}^j\rho_{-1}^n$. Two different cases can occur:

1. if the arc j is the incoming one to the supply chain (namely $a_j = -\infty$), and inflow profile $\varphi(t)$ is assigned, and we set ${}^j u_0^n = \varphi(t^n)$.
2. if the arc j is inside the supply chain, or $a_j \neq -\infty$, we set ${}^j u_0^n = \frac{T_j}{L_j} f_j^n$, where f_j^n obeys equation (1.37).

2.1.1 Correction of numerical fluxes in case of negative queues

The following lemma holds:

Lemma 27 *Consider a supply chain evolution $\rho_j(x_i, t)$, $q_j(t)$, i.e. a solution of (1.34)-(1.37). Then for every $j \in J$, $t \geq 0$ and x, it holds $\rho_j(x_i, t) \geq 0$, $q_j(t) \geq 0$.*

Since the ODE numerical scheme does not necessarily maintain the positivity proprieties of the Lemma 1, we have to modify the Euler scheme.

Consider the arc j of a supply chain and suppose that, in the time interval $\left[t^n, t^{n+1}\right[$, $\rho_j(x_i, t)$ is approximated by the constant value ${}^j\rho_i^n$. Then, from (2.2), $q_j(t)$ has a linear shape (see Fig. 2.1), namely

$$q_j(t) = \frac{q_j^{n+1} - q_j^n}{\Delta t} t + \frac{q_j^n t^{n+1} - q_j^{n+1} t^n}{\Delta t},\ t \in \left[t^n, t^{n+1}\right[. \tag{2.3}$$

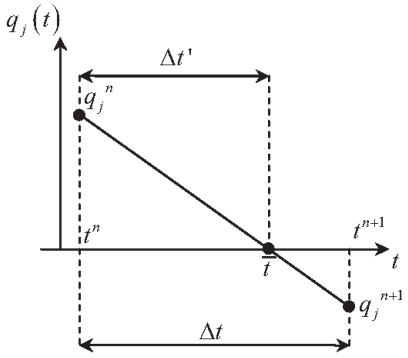

Figure 2.1: Negative queue buffer occupancy at t^{n+1}.

Assume that $q_j^n > 0$ and $q_j^{n+1} < 0$. Then, the queue vanishes at an instant of time $\bar{t} > t^n$, which is computed by (2.3):

$$\bar{t} = t^n + \Delta t',\ \Delta t' = \frac{q_j^n}{q_j^n - q_j^{n-1}} \Delta t = \frac{q_j^n}{\mu_j - f_{j-1,out}^n}.$$

Forcing to zero the behaviour of $q_j(t)$, $t \in \left[\bar{t}, t^{n+1}\right]$, the following numerical correction for the entering flux $f_{j,inc}^n$ is needed:

$$f_{j,inc}^n = \frac{1}{\Delta t}\left[\Delta t' \mu_j - \left(\Delta t - \Delta t'\right) f_{j-1,out}^n\right] \tag{2.4}$$

This correction on the boundary incoming data for the arc j influences the approximation of $\rho_j(x,t)$, with consequent effects on dynamics for following arcs and queues.

2.1.2 Different space and time grid meshes

Considering the general case in which L_j have not rational ratios, we have to consider the possibility of choosing different space and/or time grid meshes.

Different space meshes for different suppliers

For each supplier $j \in J$, the numerical grid in $[0, L_j] \times [0, T]$ is defined choosing a fixed grid mesh Δt, then different space grid meshes are necessary and we set $\Delta x_j = v_j \Delta t$, where $v_j := \frac{L_j}{T_j}$ is the processing velocity. In this case, grid points are $(x_i, t^n)_j = (i\Delta x_j, n\Delta t)$, $i = 0, ...N_j$, $n = 0, ..., \eta_j$. Then the upwind scheme for the parts density of the arc j now reads:

$$ {}^j\rho_i^{n+1} = {}^j\rho_i^n - \frac{\Delta t}{\Delta x_j} v_j \left({}^j\rho_i^n - {}^j\rho_{i-1}^n \right), \ j \in J, \ i = 0, ..., N_j, \ n = 0, ..., \eta_j. \tag{2.5} $$

To respect CFL condition (see [29]) the time mesh satisfy:

$$ \Delta t \leq \min \left\{ v_j \Delta x_j : j \in J \right\}. \tag{2.6} $$

For queues we refer again to equation (2.2).

Different time meshes for different suppliers

Now, fix two consecutive arcs $j-1$ and j. Then two different numerical grids are defined, whose points are, respectively:

$$ (x_k, t^{n_{j-1}})_{j-1} = (k\Delta x, n_{j-1}\Delta t_{j-1}), \ k = 0, ..., N_{j-1}, \ n_{j-1} = 0, ..., \eta_{j-1}, $$

$$ \left({}^jx_k, t^n \right) = (k\Delta x, n_j \Delta t_j), \ k = 0, ..., N_j, \ n_j = 0, ..., \eta_j. $$

For the queue buffer occupancy the explicit Euler is given by:

$$ q_j^{n_{j-1}} = q_j^{n_j} + \Delta t_j \left(f_{j-1,out}^{n_j} - f_{j,inc}^{n_j} \right), \tag{2.7} $$

where

$$ f_{j,inc}^{n_j} = \begin{cases} \min \left\{ f_{j-1} \left({}^{j-1}\rho_{N_{j-1}}^n \right), \mu_j \right\}, & q_j^n(t) = 0, \\ \mu_j, & q_j^n(t) > 0, \end{cases} \tag{2.8} $$

while $f_{j-1,out}^{n_j}$ must be suitably defined. If $\Delta t_{j-1} < \Delta t_j$ (see Fig.2.2), we define $m(n_j)$ and $M(n_j)$ as:

$$m\left(n_j\right) = \sup\left\{m : m\Delta t_{j-1} \leq n_j \Delta t_j\right\},$$

$$M\left(n_j\right) = \inf\left\{M : M\Delta t_{j-1} \geq \left(n_j+1\right)\Delta t_j\right\},$$

and set

$$\begin{aligned} f_{j-1,out}^{n_j} = & \sum_{l=1}^{M(n_j)-m(n_j)-1} \Delta t_{j-1} f_{j-1}\left({}^{j-1}\rho_{N_{j-1}}^{m(n_j)+l}\right) + \\ & + \left[\left(m\left(n_j\right)+1\right)\Delta t_{j-1} - n_j \Delta t_j\right] f_{j-1}\left({}^{j-1}\rho_{N_{j-1}}^{m(n_j)}\right) + \\ & + \left[\left(n_j+1\right)\Delta t_j - \left(M\left(n_j\right)-1\right)\Delta t_{j-1}\right] f_{j-1}\left({}^{j-1}\rho_{N_{j-1}}^{M(n_j)-1}\right). \end{aligned}$$

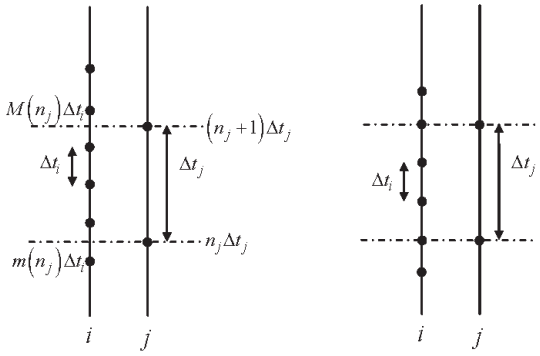

Figure 2.2: Case $\Delta t_{j-1} < \Delta t_j$. Left: not proportional case. Right: proportional case.

Notice that, in the special case $\Delta t_j = \gamma \Delta t_{j-1}$, $\gamma \in \mathbb{N} - \{1\}$, we simply have:

$$\begin{aligned} f_{j-1,out}^{n_j} = & \sum_{l=1}^{M(n_j)-m(n_j)-1} \Delta t_{j-1} f_{j-1}\left({}^{j-1}\rho_{N_{j-1}}^{m(n_j)+l}\right) = f_{j-1,out}^{n_j} = \\ & = \sum_{l=1}^{\gamma} \Delta t_{j-1} f_{j-1}\left({}^{j-1}\rho_{N_{j-1}}^{\gamma n_j+l}\right). \end{aligned}$$

If, on the contrary, $\Delta t_{j-1} > \Delta t_j$ (see Fig.2.3), we set

$$f_{j-1,out}^{n_j} = f_{j-1}^{\left\lfloor \frac{n_j \Delta t_j}{\Delta t_{j-1}} \right\rfloor},$$

where $\lfloor \cdot \rfloor$ indicates the floor function.

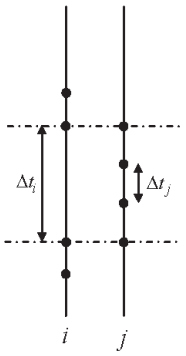

Figure 2.3: Case $\Delta t_{j-1} > \Delta t_j$.

Finally, in this case, the approximation scheme for densities is the classical upwind method.

Fluxes corrections

In case of negative values of queues, flux corrections have to be considered also for the variants of numerical method seen before.

For the modified upwind scheme, fluxes corrections are the same as in the previous section.

Now, for the modified Euler scheme for queue (2.7), we consider two consecutive arcs, $j-1$ and j, with approximation grids characterized by equal spatial meshes Δx and different temporal meshes Δt_{j-1} and Δt_j.

Assuming $q_j^{n_j} > 0$ and $q_j^{n_j+1} < 0$, if $\Delta t_{j-1} < \Delta t_j$ (see 2.4 left, for an example), more precisely $\Delta t_j = N \Delta t_{j-1}$, a possible correction for the flux entering the arc j is the following:

$$f_{j,inc}^{B} = \frac{\sum_{k=0}^{N-1} f_{j-1,out}^{k}}{N+1},$$

where f_{j-1}^k and f_j^B are, respectively, the approximations of $f_{j-1}\left(\rho_{j-1}\left(b_{j-2}, t^k\right)\right)$ and $f_j\left(\rho_j\left(a_j, t^B\right)\right)$. If $\Delta t_{j-1} > \Delta t_j$ (Fig.2.4 right), precisely $\Delta t_{j-1} = N\Delta t_j$, we indicate with $\bar{t}$ the instant such that $q_j(\bar{t}) = 0$.

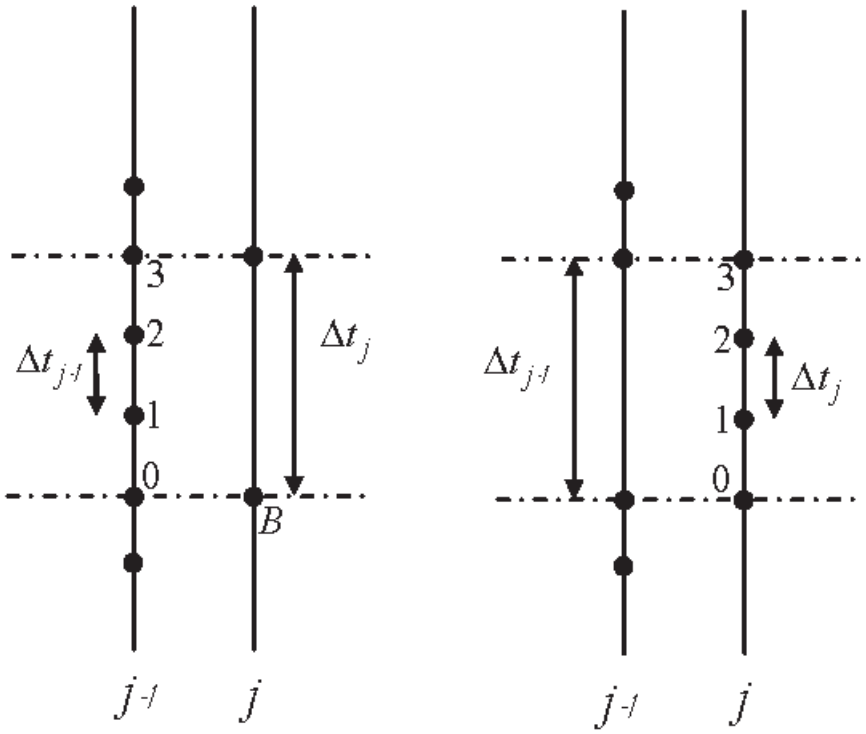

Figure 2.4: Different time meshes for fluxes corrections.

Then if

$$t^{num} = \Delta t_j \delta, \quad \text{with } \delta = \left| \frac{\bar{t}}{\Delta t_j} \right|,$$

is the numerical approximation of $\bar{t}$, a suitable correction for the flux entering the arc j can be

$$f_{j,inc}^k = \begin{cases} \mu_j, & if\ q_j\left(t^k\right) > 0, \\ \frac{\mu_j(t^{num}=\Delta t_j\delta)+[(\delta+1)\Delta t_j - t^{num}]f_{j-1,out}}{\Delta t_j}, & otherwise, \end{cases} \quad \forall k = 0, .., N-1$$

2.1.3 Convergence

According to study the convergence of the previously presented numerical schemes, the main idea is to relate the solution to those produced by Wave Front Tracking (**WFT**) and control the norm of generalized tangent vectors as in [27].

Consider the Cauchy problem of type (1.34)-(1.37), with initial conditions $\rho_{j,0}$ in the space of bounded variation functions BV. For simplicity, we consider the case of equal processing velocity and equal space and time meshes for all suppliers; the general case is similar.

Fix an initial space mesh Δx_0 and define a sequence of approximate solutions ${}^{v,j}\rho_i^n$, generated sampling the initial datum $\rho_{j,0}$ on grids of mesh $\Delta x_v = 2^{-v}\Delta x_0$ and using the time mesh:

$$\Delta t_v = v\Delta x_v = v2^{-v}\Delta x_0, \tag{2.9}$$

where v is the common velocity to all suppliers. More precisely:

$${}^{v,j}\rho_i^0 = \rho_{j,0}\left(\left(a_j + i2^{-v}\Delta x\right)+\right)$$

where $(\cdot+)$ indicates the limit from the right, which exists because of the assumption of BV initial data.

We can define a projection of the approximate solution over the space of piecewise constant functions by setting:

$$\pi_{PC}\left({}^{v,j}\rho^n\right) = \sum_{i=0}^{\frac{L_j}{2^{-v}\Delta x}-1} {}^{v,j}\rho^n \chi_{[a_j+i2^{-v}\Delta x, a_j+(i+1)2^{-v}\Delta x[}$$

where $\chi_{[a,b]}$ is the indicator function of the set $[a,b]$. Similarly we define the corresponding buffer occupancy approximations ${}^{v}q_j^n$. We will also consider the **WFT** solution ${}^{j}\rho_v^{WFT}$ starting from the initial datum:

$$\pi_{PC}\left({}^{v,j}\rho^0\right).$$

A **WFT** solution is given by:

- Solve the Riemann problems corresponding to discontinuities of $\pi_{PC}\left({}^{v,j}\rho_i^0\right)$, replacing rarefactions by a set of small non entropic shocks of size 2^{-v};

- Use the piecewise constant solution obtained piecing together the solutions to Riemann problems up to the first time of interaction of two shocks;
- Then solve a new Riemann problem created by interaction of waves and prolong the solution up to next interaction time, and so on.

In order to ensure the existence of **WFT** solutions and their convergence, it is enough to control the number of interactions, waves and the BV norm. In the scalar case, this is easily done since both number of waves and the BV norm are decreasing in time (for details [7]).

For queues we use the exact solutions to (1.35) which are indicate by ${}^{v}q_j^{WFT}$. BV estimates for complete set of *ODE-PDE* model (1.34)-(1.37) are proved in [27].

We have:

Lemma 28 *Assume that all suppliers have the common velocity v, $\rho_{j,0}$ are BV functions, $\rho_{j,0}(x) \leq \mu_j$ for every x and (2.9) holds true. Then:*

$$\left|\left|\pi_{PC}\left({}^{v,j}\rho^n\right) - {}^{j}\rho_v^{WFT}(n\Delta t_v)\right|\right|_{L^1} + \sum_j \left|{}^{v}q_j^n - {}^{v}q_j^{WFT}(n\Delta t_v)\right| \leq C2^{-v}\Delta x_0 \sum_j TV(\rho_{j,0})$$

where $C > 0$ and $TV(\cdot)$ indicates the total variation.

As in [27], we define generalized tangent vectors (v, ξ, η) to **WFT** solutions. As proved in the Lemma 2.7 of [27], the norms of tangent are decreasing along **WFT** solutions.

Now, we define the convergence error as:

$$\begin{aligned} E_v(n) &= \sum_j \sum_i 2^{-v}\Delta x_0 \left|{}^{v,j}\rho_i^n - {}^{v+1,j}\rho_i^n\right| + \sum_j \left|{}^{v}q_j^n - {}^{v+1}q_j^n\right| = \\ &= \sum_j \left|\left|\pi_{PC}\left({}^{v,j}\rho_i^n\right) - \pi_{PC}\left({}^{v+1,j}\rho_i^n\right)\right|\right|_{L^1} + \sum_j \left|{}^{v}q_j^n - {}^{v+1}q_j^n\right|. \end{aligned} \tag{2.10}$$

Moreover, we have:

$$E_v(0) = \left|\left|{}^{j}\rho_v^{WFT}(0) - {}^{j}\rho_{v+1}^{WFT}(0)\right|\right|_{L^1} \leq 2^{-(v+1)}\Delta x_0 \sum_j TV(\rho_{j,0}). \tag{2.11}$$

We can notice that the initial datum $\pi_{PC}\left({}^{v+1,j}\rho_i^0\right)$ can be obtained from $\pi_{PC}\left({}^{v,j}\rho_i^0\right)$ by possible shifting waves with tangent vectors of the $2^{v+1}\Delta x$, in fact both functions are obtained sampling the same BV function on different sub-grids.

Then, again by the Lemma 2.7 of [27], we can control the distance writing:

$$\left|\left|{}^{j}\rho_v^{WFT}(t) -^{j} \rho_{v+1}^{WFT}(t)\right|\right|_{L^1} + \sum_j \left|{}^{v}q_j^{WFT}(t) -^{v+1} q_j^{WFT}(t)\right| \leq \left|\left|{}^{j}\rho_v^{WFT}(0) -^{j} \rho_{v+1}^{WFT}(0)\right|\right|_{L^1}.$$

By the Lemma 75 and (2.11) we get:

$$\begin{aligned}
E_v(n) &= \left|\left|{}^{j}\rho_v^{WFT}(n\Delta t_v) -^{j} \rho_{v+1}^{WFT}(n\Delta t_v)\right|\right|_{L^1} + \sum_j \left|{}^{v}q_j^{WFT}(n\Delta t_v) -^{v+1} q_j^{WFT}(n\Delta t_v)\right| \\
&\quad + C\left(2^{-v} + 2^{-(v+1)}\right)\Delta x_0 \sum_j TV(\rho_{j,0}) \\
&\leq \left|\left|{}^{j}\rho_v^{WFT}(0) -^{j} \rho_{v+1}^{WFT}(0)\right|\right|_{L^1} + C\left(2^{-v} + 2^{-(v+1)}\right)\Delta x_0 \sum_j TV(\rho_{j,0}) \\
&\leq 2^{-(v+1)}\Delta x_0 \sum_j TV(\rho_{j,0}) + C\left(2^{-v} + 2^{-(v+1)}\right)\Delta x_0 \sum_j TV(\rho_{j,0}).
\end{aligned}$$

Finally we get the following:

Theorem 29 *Assume that all suppliers have the common velocity v, $\rho_{j,0}$ are BV functions, $\rho_{j,0}(x) \leq \mu_j$ for every x and (2.9) holds true. Then the convergence error $E_v(n)$ (defined in (2.10)) tends to zero uniformly in n with linear convergence rate in $\Delta x_v = 2^{-v}\Delta x_0$.*

2.2 Godunov scheme for 2×2 systems

In order to describe Godunov numerical method as applied to the system (1.47), we rewrite it as the 2×2 hyperbolic system (1.48).

The Godunov scheme is based on the construction of the Riemann problem for (1.48), $[U_L, U_R]$, which is the initial value problem for initial data given by a jump discontinuity

$$U(0,x) = \begin{cases} U_L, & x < 0, \\ U_R, & x > 0, \end{cases} \tag{2.12}$$

and it has a unique entropy solution

$$U(t,x) = U_R\left(\frac{x}{t}; U_L, U_R\right). \tag{2.13}$$

We discretize $[0,+\infty)\times\mathbb{R}$ by a time and spatial mesh length, respectively, Δt and Δx, and we let $t_n = n\Delta t$ and $x^j = j\Delta x$, so that $\left(t_n, x^j\right)$ denotes the mesh points of the approximate solution $v_\Delta(t,x) = v_n^j$. Starting by the approximation $v_n = \left(v_n^j\right)_{j\in\mathbb{Z}}$ of $U(t_n,\cdot)$, with v a column vector of $\mathbb{R}^2$, an approximation v_{n+1}^j, with $j\in\mathbb{Z}$, of $U(t_{n+1},\cdot)$ can be defined as follows:

- extension of the sequence v_n as a piecewise constant function $v_\Delta(t,\cdot)$:

$$v_\Delta(t,\cdot) = v_n^j, \quad x^{j-\frac{1}{2}} < x < x^{j+\frac{1}{2}}; \tag{2.14}$$

  solution of the Cauchy problem

$$\begin{cases} U_t + F(U)_x = 0, & x\in\mathbb{R},\ t>0, \\ U(0,x) = v_\Delta(t_n,\cdot), \end{cases} \tag{2.15}$$

  in the cell $(t_n, t_{n+1})\times\left(x^{j-1}, x^j\right)$;

- computation of the solution as the average value of the preceding solution in the interval $\left(x^{j-\frac{1}{2}}, x^{j+\frac{1}{2}}\right)$ obtained projecting $U(\Delta t,\cdot)$ onto the piecewise constant functions:

$$v_{n+1}^j = \frac{1}{\Delta x}\int_{x^{j-\frac{1}{2}}}^{x^{j+\frac{1}{2}}} U(\Delta t, x)\, dx. \tag{2.16}$$

To avoid the interaction of waves in two neighbouring cells before time Δt, we impose a CFL(*Courent-Friedrichs-Lewy*) condition as:

$$\frac{\Delta t}{\Delta x}\max\{|\lambda_0|, |\lambda_1|\} \le \frac{1}{2}, \tag{2.17}$$

where λ_0 and λ_1 are the eigenvalues. Since, in this case, we have that $|\lambda_0| = 1$ and $|\lambda_1| \le 1$, the CFL condition reads as:

$$\frac{\Delta t}{\Delta x} \le \frac{1}{2}.$$

The solution of (2.15) is obtained by solving a sequence of neighbouring Riemann problems and we have

$$U(t,x) = U_R\left(\frac{x - x^{j+\frac{1}{2}}}{\Delta t}; v_n^j, v_n^{j+1}\right),\ x^j < x < x^{j+1},\ j \in \mathbb{Z}. \tag{2.18}$$

Then, a more explicit expression of the scheme can be obtained integrating the equation (2.15) over the rectangle $(0, \Delta t) \times \left(x^{j-\frac{1}{2}}, x^{j+\frac{1}{2}}\right)$. Since the function is piecewise smooth, we get:

$$\int_{x^{j-\frac{1}{2}}}^{x^{j+\frac{1}{2}}} \left(U(\Delta t, 0) - U(0,x)\right) dx +$$

$$+ \int_0^{\Delta t} \left(F\left(U\left(t, x^{j+\frac{1}{2}} - 0\right)\right) - F\left(U\left(t, x^{j-\frac{1}{2}} + 0\right)\right)\right) dt = 0.$$

Now, using (2.14) and projecting the solution on piecewise constant functions we obtain:

$$\Delta x\left(v_{n+1}^j - v_n^j\right) + \int_0^{\Delta t} \left(F\left(U\left(t, x^{j+\frac{1}{2}} - 0\right)\right) - F\left(U\left(t, x^{j-\frac{1}{2}} + 0\right)\right)\right) dt = 0 \tag{2.19}$$

and, recalling (2.18), we derive:

$$v_{n+1}^j = v_n^j - \frac{\Delta t}{\Delta x}\left\{F\left(U_R\left(0-; v_n^j, v_n^{j+1}\right)\right) - F\left(U_R\left(0+; v_n^{j-1}, v_n^j\right)\right)\right\}. \tag{2.20}$$

Since the function $\xi \to F\left(U_R\left(\xi; U_L, U_R\right)\right)$ is continuous at the origin due to the Rankine-Hugoniot conditions (see [22]), Godunov scheme can be written in the form:

$$v_{n+1}^j = v_n^j - \frac{\Delta t}{\Delta x}\left\{F\left(U_R\left(0; v_n^j, v_n^{j+1}\right)\right) - F\left(U_R\left(0; v_n^{j-1}, v_n^j\right)\right)\right\}, \tag{2.21}$$

and the numerical flux computed in $V = (v_1, v_2)$ and $W = (w_1, w_2)$, is

$$G(V,W) = F\left(U_R(0; V, W)\right). \tag{2.22}$$

The numerical flux can be written in a general form as:

$$G(V,W) = \begin{cases} \min_{z_1 \in [v_1, w_1]} F(Z) & \text{if } v_1 \le w_1 \\ \max_{z_1 \in [v_1, w_1]} F(Z) & \text{if } v_1 \ge w_1 \end{cases}$$

where the second variable z_2 in $Z = (z_1, z_2)$ is assumed to be fixed. The final expression of Godunov scheme for the problem (2.15) is:

$$v_{n+1}^j = v_n^j - \frac{\Delta t}{\Delta x}\left(G\left(v_n^j, v_n^{j+1}\right) - G\left(v_n^{j-1}, v_n^j\right)\right). \tag{2.23}$$

More precisely, for the system (1.48), the scheme reads as:

$$\begin{cases} \rho_{n+1}^j = \rho_n^j - \frac{\Delta t}{\Delta x}\left(g\left(\rho_n^j, \rho_n^{j+1}\right) - g\left(\rho_n^{j-1}, \rho_n^j\right)\right), \\ \mu_{n+1}^j = \mu_n^j - \frac{\Delta t}{\Delta x}\left(\mu_{n+1}^j - \mu_n^j\right), \end{cases} \tag{2.24}$$

where the approximate values of $\rho(x,t)$ and $\mu(x,t)$ on the numerical grid is indicated as, respectively, ρ_n^j and μ_n^j for $j = 0, ..., L$ and $n = 0, ..., M-1$. In the (2.24) we can observe that the Godunov scheme for the second equation reduces to forward upwind scheme.

2.2.1 Fast Godunov for 2×2 system

In order to find a simplified expression for the numerical flux of Godunov scheme, considering as numerical flux the function $F(U)$ with $f(\rho, \mu)$ defined in (1.47), we solve Riemann problems between the two states: (ρ_-, μ_-) on the left and (ρ_+, μ_+) on the right. In particular, referring to relation (2.22), we compute the value of $F(U)$ in the separation point between waves of different speed.

Theorem 30 *The numerical flux function* $G(V, W) = F(U_R(0; V, W))$ *is*

$$G(\rho_-, \mu_-, \rho_+, \mu_+) = \begin{cases} (\rho_-, -\mu_+) & \text{if } \rho_- < \mu_- \vee \rho_- \leq \mu_+, \\ \left(\frac{1-\varepsilon}{1+\varepsilon}\mu_+ + \frac{2\varepsilon}{1+\varepsilon}\rho_-, -\mu_+\right) & \text{if } \rho_- < \mu_- \vee \rho_- > \mu_+, \\ \left(\frac{1+\varepsilon}{2}\rho_- + \frac{1-\varepsilon}{2}\mu_-, -\mu_+\right) & \text{if } \rho_- \geq \mu_- \vee \mu_+ > \tilde{\mu}, \\ \left(\frac{1-\varepsilon}{1+\varepsilon}(\mu_+ + \varepsilon\mu_-) + \varepsilon\rho_-, -\mu_+\right) & \text{if } \rho_- \geq \mu_- \vee \mu_+ \leq \tilde{\mu}, \end{cases} \tag{2.25}$$

with

$$\tilde{\mu} = \mu_- + \frac{1+\varepsilon}{2}(\rho_- - \mu_-). \tag{2.26}$$

Proof. Let P be the intersection point between the first family curve passing through (ρ_-, μ_-) and the line $\rho = \mu$, namely $P = \begin{pmatrix} \rho_- \\ \rho_- \end{pmatrix}$. The second family curve passing through P splits the invariant region into two regions $A =$

$\{(\rho,\mu) : \mu > \rho_-\}$ and $B = \{(\rho,\mu) : \mu \leq \rho_-\}$ as shown in Fig.2.5 and Fig.2.6. Each Riemann problem solution presents waves traveling with two velocities, namely $\lambda_0 = -1$ and $0 < \varepsilon \leq \lambda_1 \leq 1$. If (ρ_*, μ_*) is the intermediate state (see Fig.2.7), we compute the numerical flux function $G(\rho_-, \rho_+)$ given by $(f(\rho_*, \mu_*), \mu_*)$. We distinguish two different cases:

Case1: $\rho_- < \mu_-$. In this case, if $(\rho_+, \mu_+) \in A$ then $(\rho_*, \mu_*) = (\rho_-, \mu_+)$. If $(\rho_+, \mu_+) \in B$, the needed value of flux is that corresponding to $(f(\rho_*, \mu_+), -\mu_+)$ (see Fig.2.5). We have

$$(\rho_*, \mu_*) = (\rho_*, \mu_+) = \begin{pmatrix} \rho_- \\ \rho_- \end{pmatrix} + t \begin{pmatrix} -\frac{1-\varepsilon}{1+\varepsilon} \\ \rho_- \end{pmatrix} \tag{2.27}$$

and ρ_* is computed as:

$$\rho_* = \rho_- + (\rho_- - \mu_+)\frac{1-\varepsilon}{1+\varepsilon}. \tag{2.28}$$

Finally, since $\rho_* > \rho_- > \mu_+$ we get the expression in the second line of (2.25).

Case 2: $\rho_- \geq \mu_-$. In this case, if $(\rho_+, \mu_+) \in A$ then $(\rho_*, \mu_*) = (\tilde{\rho}, \mu_+)$, where

$$\tilde{\rho} = \frac{1+\varepsilon}{2}\rho_- + \frac{1-\varepsilon}{2}\mu_- \tag{2.29}$$

is obtained as follows. The point $(\tilde{\rho}, \tilde{\mu})$ is:

$$(\tilde{\rho}, \tilde{\mu}) = \begin{pmatrix} \rho_- \\ \mu_- \end{pmatrix} + t \begin{pmatrix} -\frac{1-\varepsilon}{1+\varepsilon} \\ 1 \end{pmatrix},$$

and, using that $\tilde{\rho} = \tilde{\mu}$, it is possible to get (2.29). Assuming $(\rho_+, \mu_+) \in B$, the value of flux we need is $f(\rho_*, \mu_+)$ with ρ_* given by

$$(\rho_*, \mu_*) = (\rho_*, \mu_+) = \begin{pmatrix} \rho_- \\ \mu_- \end{pmatrix} + t \begin{pmatrix} -\frac{1-\varepsilon}{1+\varepsilon} \\ 1 \end{pmatrix}, \tag{2.30}$$

and, making simple computations, one gets:

$$\rho_* = \rho_- + (\mu_- - \mu_+)\frac{1-\varepsilon}{1+\varepsilon}. \tag{2.31}$$

Taking into account that $\rho_* > \mu_+$, we obtain the expression of flux as in the last line of (2.25).

■

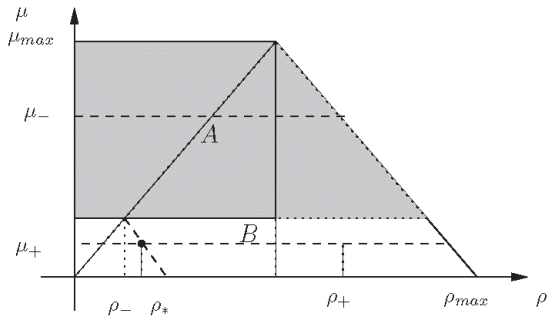

Figure 2.5: Case 1, with $(\rho_+, \mu_+) \in B$.

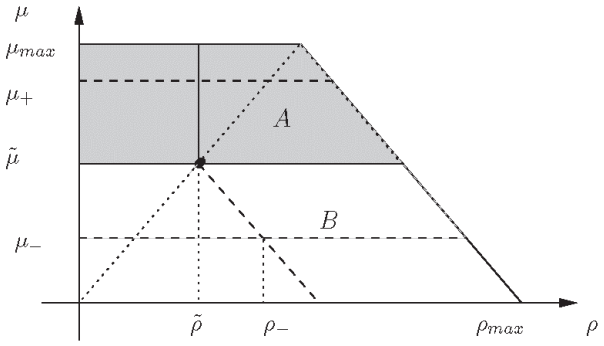

Figure 2.6: Case 2, with $(\rho_+, \mu_+) \in A$.

2.3 Numerics for Riemann Solvers

In this sub-section, in order to describe the numerical framework for the solution of Riemann problems at junctions, we refer to the general Riemann solver called **SC1** [14] and to **SC2** and **SC3**.

For simplicity, we focus on a single supplier v^e, and on two consecutive sub-chains, e and $e+1$.

Let us introduce the following notations:

- $\rho_n^{e,L}$,$\mu_n^{e,L}$ are the approximate values, respectively, of density and processing rate at time t_n at the outgoing endpoint $x_L = L\Delta x$ of sub-chain e;

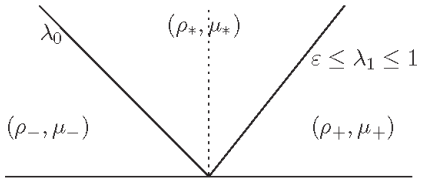

Figure 2.7: Intermediate state between the two waves.

- $\rho_n^{e,0}$,$\mu_n^{e,0}$ are the approximate values, respectively, of density and processing rate at time t_n at the incoming endpoint $x_0 = 0$ of sub-chain $e+1$;

2.3.1 Discretization of the Riemann Solver SC1

Setting

- $\hat{\gamma} = f\left(\rho_n^{e,L}, \mu_n^{e,L}\right)$,
- $\gamma_{\max}^{e+1} = f\left(\rho_{\max}^{e}, \mu_n^{e+1,0}\right)$,

we consider two cases:

Case α) If $\hat{\gamma} \leq \gamma_{\max}^{e+1}$:

$$\rho_n^{e,L+1} = \rho_n^{e,L},$$

$$\mu_n^{e,L+1} = \mu_n^{e,L},$$

$$\rho_n^{e+1,-1} = \begin{cases} f\left(\rho_n^{e,L}, \mu_n^{e,L}\right) & \text{if } f\left(\rho_n^{e,L}, \mu_n^{e,L}\right) \leq \mu_n^{e+1,0}, \\ \frac{f\left(\rho_n^{e,L}, \mu_n^{e,L}\right) - \mu_n^{e+1,0}}{\varepsilon} - \mu_n^{e+1,0} & otherwise, \end{cases}$$

$$\mu_n^{e+1,-1} = \mu_n^{e+1,0};$$

Case β) If $\hat{\gamma} > \gamma_{\max}^{e+1}$:

$$\rho_n^{e,L+1} = \rho_n^{e,L},$$

$$\mu_n^{e,L+1} = \frac{\gamma_{\max}^{e+1} - \varepsilon \rho_n^{e,L}}{1-\varepsilon},$$

$$\rho_n^{e+1,-1} = \rho_{\max}^{e},$$

$$\mu_n^{e+1,-1} = \mu_n^{e+1,0}.$$

2.3.2 Discretization of the Riemann Solver SC2

Case α) We have two subcases:

α_1) if $\rho^* < \rho_M$, we set:

$$\rho_n^{e,L+1} = \rho_n^{e,L},$$
$$\mu_n^{e,L+1} = \min\left\{\rho^*, \mu_{\max}^e\right\},$$
$$\rho_n^{e+1,-1} = \rho^*,$$
$$\mu_n^{e+1,-1} = \mu_n^{e+1,0};$$

α_2) if $\rho^* \geq \rho_M$, the new values are:

$$\rho_n^{e,L+1} = \rho_n^{e,L},$$
$$\mu_n^{e,L+1} = \varepsilon\frac{1+\varepsilon}{1-\varepsilon}\tilde{\rho} - \frac{2\varepsilon}{1-\varepsilon}\bar{\mu}^e + (1+\varepsilon)\,\mu_n^{e+1,0},$$
$$\rho_n^{e+1,-1} = \tilde{\rho},$$
$$\mu_n^{e+1,-1} = \mu_n^{e+1,0};$$

Case β)

$$\rho_n^{e,L+1} = \rho_n^{e,L},$$
$$\mu_n^{e,L+1} = \bar{\mu}^e,$$
$$\rho_n^{e+1,-1} = \bar{\mu}^e,$$
$$\mu_n^{e+1,-1} = \mu_n^{e+1,0}.$$

2.3.3 Discretization of the Riemann Solver SC3

Case α) two subcases occur:

α_1) if $\rho^* < \rho_M$, we set:

$$\rho_n^{e,L+1} = \rho_n^{e,L},$$
$$\mu_n^{e,L+1} = \max\left\{\rho^*, \mu_n^{e,L}\right\},$$
$$\rho_n^{e+1,-1} = \rho^*,$$
$$\mu_n^{e+1,-1} = \mu_n^{e+1,0};$$

α_2) if $\rho^* \geq \rho_M$, we compute the new values as in **SC2**:

$$\rho_n^{e,L+1} = \rho_n^{e,L},$$
$$\mu_n^{e,L+1} = \varepsilon \frac{1+\varepsilon}{1-\varepsilon}\tilde{\rho} - \frac{2\varepsilon}{1-\varepsilon}\bar{\mu}^e + (1+\varepsilon)\,\mu_n^{e+1,0},$$
$$\rho_n^{e+1,-1} = \tilde{\rho},$$
$$\mu_n^{e+1,-1} = \mu_n^{e+1,0};$$

Case β)

$$\rho_n^{e,L+1} = \rho_n^{e,L},$$

β_1) if $\mu_n^{e,L+1} \geq \bar{\mu}^e$, we set:

$$\mu_n^{e,L+1} = \mu_n^{e,L},$$

β_2) otherwise, we assign:

$$\mu_n^{e,L+1} = \bar{\mu}^e,$$
$$\rho_n^{e+1,-1} = \bar{\mu}^e,$$
$$\mu_n^{e+1,-1} = \mu_n^{e+1,0}.$$

Chapter 3

Simulations

In this section, first, we report some numerical results analyzing the use of the Klar model and the continuum-discrete model for supply chain. Then we will compare, via simulations, performances between the two previous model showing some differences.

Moreover, we report the behaviour of a supply chain network based on both models.

Finally we discuss about some optimization techniques related to Klar model for supply chain.

3.1 Numerical results

3.1.1 An example of supply chain network with more incoming and outgoing subchains

Göttlich-Herty-Klar model for supply chain network

Consider the supply chain with four arcs represented in figure 3.1.

It consists of seven processors with queues characterized by length L_j, capacity μ_j, processing time T_j, and the distribution coefficient α_j for $j = 1, .., 7$ and an inflow arc. Then we summarize these quantities for each processor in the following

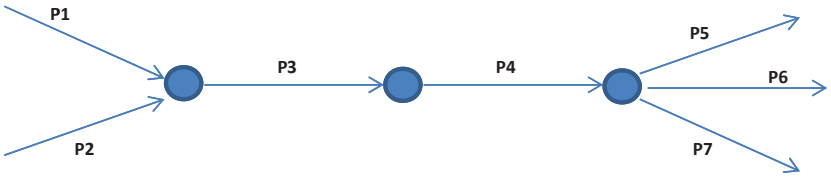

Figure 3.1: A simple network.

table:

Processor j	μ_j	T_j	L_j	α_j
$P1$	1	0.4	1	0.8
$P2$	1.5	0.2	0.2	0.2
$P3$	2	1	1	1
$P4$	3	1	0.5	1
$P5$	0.5	1	1	0.4
$P6$	0.8	1	1	0.5
$P7$	1.2	1	0.2	0.1

We suppose that at time $t = 0$, all arcs are empty, i.e. $\rho_{j,0} = 0\ \forall x \in [0, L_j]$ and the queues are assumed zero, i.e. $q_{j,0} = 0$, $j = 3, 4, 5, 6, 7$. The initial inflow profile for processors $P1$ and $P2$ is the same and is given by the following expression:

$$f_{1,2}(t) = \begin{cases} \frac{18}{35}t, & 0 \leq t \leq 10, \\ 36 - \frac{18}{35}t, & 10 < t \leq 18, \\ 20, & 18 < t \leq T. \end{cases} \tag{3.1}$$

Let assume a total simulation time $T = 30$ and discretization spatial and time step constants for each arc, respectively $\Delta x = 0.02$ and $\Delta t = 0.1$ (such that the CFL condition is satisfied). The output solution queue at the last node have only two components due to processors $P5$ and $P6$, while $P7$ has not queue component(Fig. 3.2).

In figure 3.3 it shows the evolutionary behaviour of the density on each output processor. We have to notice that after a period of increasing, the density remains constant to the value of maximum capacity as we expect.

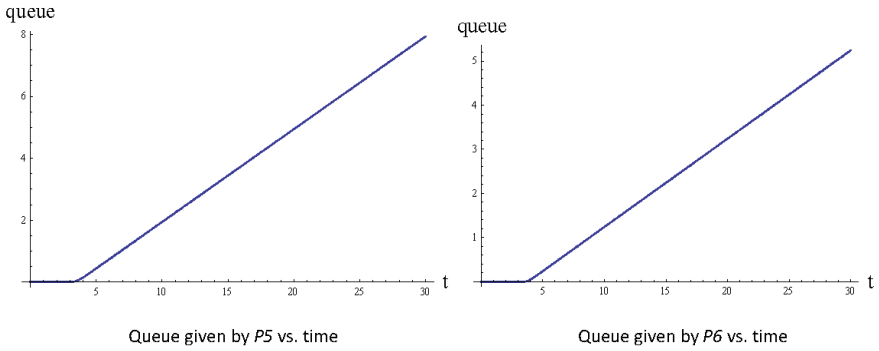

Figure 3.2: queue values vs. time given by processors *P5* and *P6*.

Continuum-discrete model for supply chain

In order to compare the continuum-discrete model and the Klar model, we refer to the previous example considering the flux function with different slopes m_k (see **Remark 54**). The expression of numerical flux $G(\rho_-, \mu_-, \rho_+, \mu_+)$ of fast Godunov scheme for supplier I_k is:

$$G = \begin{cases} (m_k\rho_-, -\mu_+) & \text{if } \rho_- < \mu_- \vee \rho_- \leq \mu_+, \\ \left(\left(m_k - \frac{2\varepsilon}{1+\varepsilon}\right)\mu_+ + \frac{2\varepsilon}{1+\varepsilon}\rho_-, -\mu_+\right) & \text{if } \rho_- < \mu_- \vee \rho_- > \mu_+, \\ \left(m_k\left(\frac{1+\varepsilon}{2}\rho_- + \frac{1-\varepsilon}{2}\mu_-\right), -\mu_+\right) & \text{if } \rho_- \geq \mu_- \vee \mu_+ > \tilde{\mu}, \\ \left(\left(m_k - \frac{2\varepsilon}{1+\varepsilon}\right)\mu_+ + \frac{1-\varepsilon}{1+\varepsilon}\varepsilon\mu_- + \varepsilon\rho_-, -\mu_+\right) & \text{if } \rho_- \geq \mu_- \vee \mu_+ \leq \tilde{\mu}, \end{cases} \tag{3.2}$$

with $\tilde{\mu}$ as in (2.26). Then, we have again $N = 7$ processors described by the following table:

Processor k	μ_k	L_k	m_k	α_j
$P1$	1	1	1	0.8
$P2$	1.5	0.2	0.2	0.2
$P3$	2	1	1	1
$P4$	3	0.5	1	1
$P5$	0.5	1	0.2	0.4
$P6$	0.8	1	0.2	0.5
$P7$	1.2	0.2	0.5	0.1

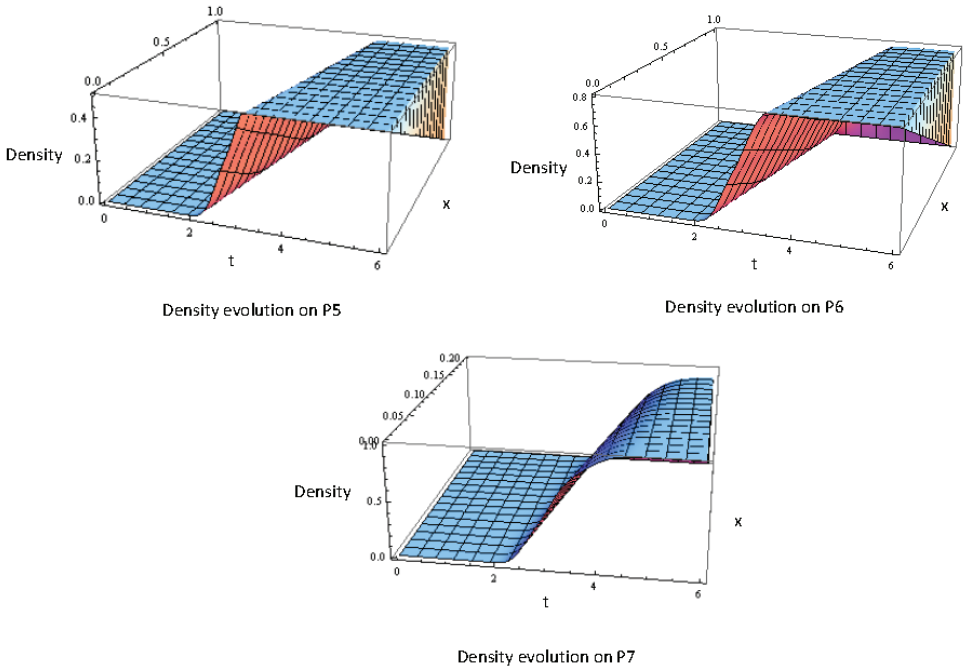

Figure 3.3: density values vs. time and space of processors *P5*, *P6* and *P7*.

Let us assume the initial data as $\rho_k(t,x) = 0$, $k = 1,..,7$ and the boundary data, for both the processors $P1$ and $P2$, is still given by 3.1.

The simulation time is assumed to be $T = 30$, with $\Delta x = 0.02$ and $\Delta t = 0.01$.

The evolution in time and space of density, considering the Riemann Solver **SC2** for $\varepsilon = 0.2$ is shown in Fig. 3.4.

3.1.2 Example of a network with one incoming and outgoing sub-chain

Let consider the supply chain network, with 8 processors as in Fig. 3.5.

We assume the following quantities for each processor.

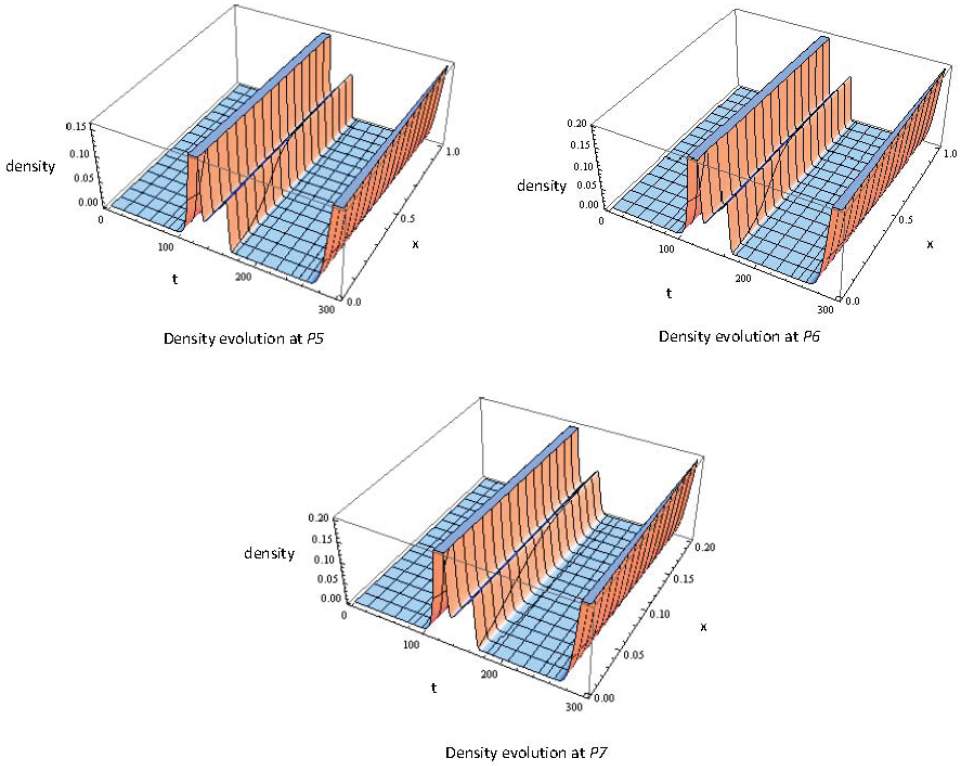

Figure 3.4: density values vs. time and space of processors *P5*, *P6* and *P7*.

Processor j	$\mu_{\max}$	T_j	L_j	α_j
$P1$	1.3	1.5	1.5	1
$P2$	2.5	3	3	0.3
$P3$	2	1	1	0.7
$P4$	1.2	1.5	1.5	1
$P5$	1	2	2	1
$P6$	1.5	2	2	0.2
$P7$	1	2	2	0.8
$P8$	0.2	1	1	1

Let assume that at time $t = 0$ $\rho_{j,0} = 0$ $\forall x \in [0, L_j]$ and $q_{j,0} = 0$, $j = 3, 4, 5, 6, 7$. The initial inflow profile for processors $P1$ is given by

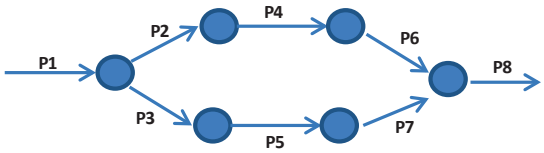

Figure 3.5: A network with 8 processors.

$$f_1(t) = \begin{cases} 100, & 0 \leq t \leq 500, \\ 120, & 500 < t \leq T, \end{cases}$$

where $T = 1000$. To satisfy the CFL condition we assume $\Delta x = 0.2$ and $\Delta t = 0.1$. Then, considereing the Göttlich-Herty-Klar model, the output queue and the density on processor $P8$ is represented in figures, respectively, Fig. 3.6 and Fig. 3.7.

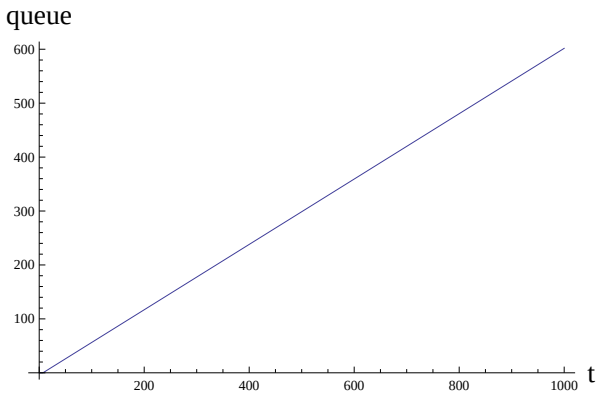

Figure 3.6: queue values vs. time at processors *P8*.

Instead, according to the continuum-discrete model we obtain the behavior of density on processor $P8$ as in Fig. 3.8.

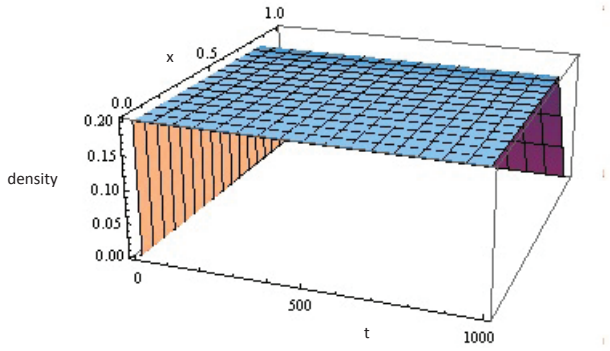

Figure 3.7: density values vs. time and space at processors *P8*.

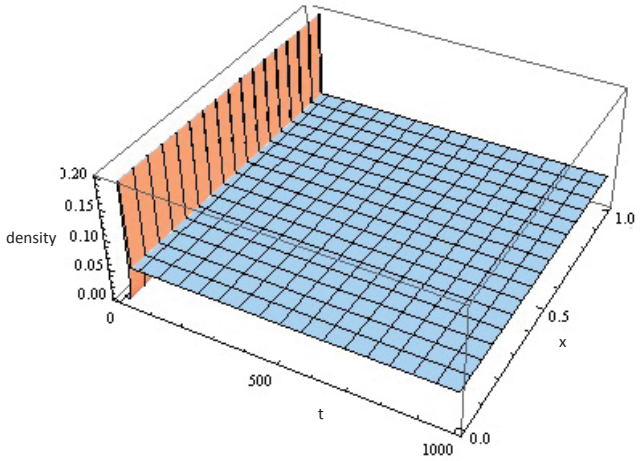

Figure 3.8: density values vs. time and space at processors *P8*.

Bibliography

[1] E. J. Anderson, *A new continuous model for job shop scheduling*, International J Systems Science 12: 1469-1475 (1981).

[2] D. Armbruster, P. Degond and C. Ringhofer, *A model for the dynamics of large queuing networks and supply chains.*, SIAM J. Appl. Math., 66 (2006), pp. 896-920.

[3] D. Armbruster, D. Marthaler, C. Ringhofer, *Kinetic and fluid model hierarchies for supply chains*, SIAM J. on Multiscale Modeling, 2 (1), pp. 43 - 61, 2004.

[4] C. Bardos, A.Y. Le Roux, J.C. Nedelec, *First order quasilinear equations with boundary conditions*, Comm. Partial Differential Equations, 4 pp. 1017-1034, (1979).

[5] W.-J. Baumol, *Economic Dynamics*, Macmilan, New York, 1970.

[6] R. Billings, J. Hasenbein, *Applications of fluid models to semiconductor fab operations*, preprint, (2001).

[7] A. Bressan, *Hyperbolic Systems of Conservation Laws*, Oxford Univ. Press, 2000.

[8] A. Bressan, G. Crasta, B. Piccoli, *Well Posedness of the Cauchy Problem for $n \times n$ Systems of Conservation Laws*, Memoirs of the American Mathematical Society, vol. 146, n. 694, 2000.

[9] G. Bretti, C. D'Apice, R. Manzo and B. Piccoli, *A continuum-discrete model for supply chains dynamics*, Networks and Heterogeneous Media, (2007).

[10] C. Dafermos, *Hyperbolic Conservation Laws in Continuum Physics*, Springer - Verlang, 1999.

[11] C.F. Daganzo, *A continuum theory of traffic dynamics for freeways with special lanes*, Trans. Res. B, 31 (1997), p. 83.

[12] C.F. Daganzo, *A Theory of Supply Chains*, Springer Verlang, New York, Berlin, Heidelberg, 2003.

[13] Y. Dallery and S.B. Gershwin, *Manufacturing flow line systems: A review of models and analytical results*, Queueing Systems, 12, pp. 3-94, 1992.

[14] C. D'Apice, R. Manzo, *A fluid-dynamic model for supply chain*, Networks and Heterogeneous Media (NHM) (2006), Vol. 1, No. 3, pp. 379-398.

[15] C. D'Apice, R. Manzo, B. Piccoli, *Modelling supply networks with partial differential equations*, submitted to CMS.

[16] P. Degond, S. Göttlich, M. Herty and A. Klar, *A network model for supply chains with multiple policies*, SIAM J. on Multiscale Models, (2007).

[17] J. P. Dias, M. Figueira, *On the Riemann problem for some discontinuous systems of conservation laws describing phase transitions*, Commun. Pure Appl. Anal., 3, pp. 53-58 (2004).

[18] J. P. Dias, M. Figueira, *On the approximation of the solutions of the Riemann problem for a discontinuous conservation law*, Bull. Braz. Math. Soc. (N.S.), 36, pp. 115-125 (2005).

[19] J. P. Dias, M. Figueira, *On the viscous Cauchy problem and the existence of shock profiles for a p-system with a discontinuous stress function*, Quart. Appl. Math., 63, pp. 335-341 (2005).

[20] J. P. Dias, M. Figueira, J.F. Rodrigues, *Solutions to a scalar discontinuous conservation law in a limit case of phase transitions*, J. Math. Fluid Mech., 7, pp. 153-163 (2005).

[21] J. W. Forrester, *Industrial Dynamics*, MIT Press, MA, 1964.

[22] E. Godlewski and P.A. Raviart, *Hyperbolic systems of conservation laws*, Mathématiques & Applications [Mathematics and Applications], 3/4. Ellipses, Paris, 1991.

[23] S. Göttlich, M. Herty and A. Klar, *Modelling and optimization of Supply Chains on Complex Networks*, Communication in Mathematical Sciences, 4(2), pp. 315-330, 2006.

[24] D. Helbing, D. Armbruster, A. Mikhailov and E. Lefeber, *Information and material flows in complex networks*, Physica A, 363 (2006).

[25] D. Helbing, S. Lammer, *Supply and production networks: from the bullwhip effect to business cycles*, in: D. Armbruster, A. S. Mikhailov and K. Kaneko (eds.) *Networks of Interacting Machines: Production Organization in Complex Industrial Systems and Biological Cells*, World Scientific, Singapore, 2005, pp. 33-66.

[26] D. Helbing, S. Lammer, T. Seidel, P. Seba, T. Platkowski, *Physics, stability and dynamics of supply networks*, Physical Review E 70 (2004), 066116.

[27] M. Herty, A. Klar, B. Piccoli, *Existence of solutions for supply chain model based on partial differential equations*, SIAM J. Math. An., 39(1), pp. 160-173, 2007.

[28] S. N. Kruzkov, *First order quasi linear equations in several independent variables*, Math. USSR Sbornik, 10 (1970), p. 217.

[29] R. J. Leveque, *Finite Volume Methods for Hyperbolic Problems*, Cambridge, 2002.

[30] J. Little, *A proof for the queueing formula* $l = \lambda\varpi$, Operations Research, 9, pp.383-387, 1961.

[31] G. F. Newell, *A simplified theory of kinematic waves in highway traffic*, Transportation Research B, 27 (1993), pp. 281-313.